



## King's Research Portal

DOI:

[10.1016/j.fss.2024.109155](https://doi.org/10.1016/j.fss.2024.109155)

*Document Version*

Peer reviewed version

[Link to publication record in King's Research Portal](#)

*Citation for published version (APA):*

Han, M., Huang, Y., Guo, G., Lam, H.-K., & Wang, Z. (2025). Estimation of the Domain of Attraction for Continuous-Time Saturated Positive Polynomial Fuzzy Systems Based on Novel Analysis and Convexification Strategies. *Fuzzy Sets and Systems*, 498, Article 109155. <https://doi.org/10.1016/j.fss.2024.109155>

### **Citing this paper**

Please note that where the full-text provided on King's Research Portal is the Author Accepted Manuscript or Post-Print version this may differ from the final Published version. If citing, it is advised that you check and use the publisher's definitive version for pagination, volume/issue, and date of publication details. And where the final published version is provided on the Research Portal, if citing you are again advised to check the publisher's website for any subsequent corrections.

### **General rights**

Copyright and moral rights for the publications made accessible in the Research Portal are retained by the authors and/or other copyright owners and it is a condition of accessing publications that users recognize and abide by the legal requirements associated with these rights.

- Users may download and print one copy of any publication from the Research Portal for the purpose of private study or research.
- You may not further distribute the material or use it for any profit-making activity or commercial gain
- You may freely distribute the URL identifying the publication in the Research Portal

### **Take down policy**

If you believe that this document breaches copyright please contact [librarypure@kcl.ac.uk](mailto:librarypure@kcl.ac.uk) providing details, and we will remove access to the work immediately and investigate your claim.

# Estimation of the Domain of Attraction for Continuous-Time Saturated Positive Polynomial Fuzzy Systems Based on Novel Analysis and Convexification Strategies

Meng Han<sup>a</sup>, Yongjie Huang<sup>a</sup>, Ge Guo<sup>a,b,\*</sup>, H. K. Lam<sup>c</sup> and Zhengsong Wang<sup>a</sup>

<sup>a</sup>School of Information Science and Engineering, Northeastern University, Shenyang 110819, China

<sup>b</sup>State Key Laboratory of Synthetical Automation for Process Industries, Northeastern University, Shenyang 110819, China

<sup>c</sup>Department of Engineering, King's College London, WC2R 2LS London, U.K.

## ARTICLE INFO

### Keywords:

Positive polynomial fuzzy systems  
input saturation  
advanced Chebyshev-membership-  
functions-dependent method  
imperfect premise matching (IPM)  
concept  
domain of attraction (DOA)  
linear copositive Lyapunov function

## ABSTRACT

In this paper, the domain of attraction (DOA) of the continuous-time positive polynomial fuzzy systems subject to input saturation is estimated by using the level set of the linear copositive Lyapunov function. To relax the estimation of DOA, the restriction on the level set is removed by embedding the expression of the level set into the stability conditions and positivity conditions. Referring to the nonconvex terms caused by above novel analysis strategy, some polynomial inequality lemmas are proposed to handle them; the nonconvex terms caused by imperfect premise matching (IPM) nonlinear membership functions are dealt with by sector nonlinear methods and advanced Chebyshev membership-function-dependent (MFD) methods. In this advanced MFD method, the state space segmentation and polynomial order selection of the Chebyshev approximation method are improved based on breakpoints of the first derivative and curvature, respectively, which is helpful to reduce the conservatism and computational burden of the result. Thus, this advanced Chebyshev MFD method not only optimizes the convexification strategy, but also can further be extended to estimate the DOA when it is used to introduce the membership functions information for convex stability and positivity conditions. Finally, a numerical example and the lipoprotein metabolism and potassium ion transfer nonlinear model are presented to validate the effectiveness and feasibility of the aforementioned analysis and convexification strategies in the expansion of DOA estimation.

## 1. INTRODUCTION

If the system states of a dynamic system are nonnegative, such as population quantity [1], traffic flow [2], material concentration [3] and so on, the nonnegative constraints on these system states cannot be accurately represented by the general systems, so the positive systems whose state trajectories are confined to positive quadrant are proposed to make up for the shortcomings of general systems in modeling dynamic systems with nonnegative variables [4]. Due to these special properties, research on positive systems has attracted wide attention, but most of the research results are only applicable to linear positive systems [5–8] and cannot be directly extended to nonlinear positive systems. However, nonlinear dynamics are included in almost all real-world systems, which motivates us to conduct systematic analysis and control synthesis of nonlinear positive systems.

Due to the combined effect of nonlinear dynamics and positive constraints, the study of nonlinear positive systems is extremely difficult and progresses slowly [9–12]. Fortunately, the Takagi-Sugeno (T-S) fuzzy model [13] and the polynomial fuzzy model [14] have emerged as effective tools for handling nonlinear terms, and they can model nonlinear positive systems as convex combination systems of linear or polynomial sub-systems weighted by nonlinear membership functions [15–22], which greatly reduces the difficulty of the research on nonlinear positive systems. Compared to the T-S fuzzy model, the polynomial fuzzy model allows polynomials to appear in the subsystems, thus providing a stronger modeling capability for nonlinear positive systems. When performing the control synthesis for fuzzy-model-based nonlinear positive plants, the premise membership functions of the controller can be designed to be different from those of the plants, which is called the imperfect premise matching (IPM) controller design strategy [23]. Although the IPM controller design strategy will bring more difficulty than the traditional parallel distributed

\*Corresponding author

✉ hanmeng@neuq.edu.cn (M. Han); 2201996@stu.neu.edu.cn (Y. Huang); geguo@yeah.net (G. Guo); hak-keung.lam@kcl.ac.uk (H.K. Lam); zswang\_pine@126.com (Z. Wang)

compensation (PDC) controller design strategy in theoretical analysis, it can effectively reduce the implementation cost of the fuzzy controller when the premise membership functions of the fuzzy plants are complex.

In practical systems, input saturation is a common phenomenon. For the systems subject to input saturation, the conservatism of dealing with the saturation function will affect the estimated size of **the domain of attraction (DOA)** which refers to the region of system states that can be controlled. In order to expand the estimation of DOA, some **literature** has been devoted to proposing low-conservative approaches to handle the saturation function, such as the sector-condition-based method [24], the convex hull representation method and its improved versions [25–27], the inequality representation method [7], and so on. In [7], the inequality representation method is adopted, and the level set of the linear copositive Lyapunov function [28] that is used to estimate DOA of positive systems is embedded in the stability conditions and positivity conditions with the help of the  $S$ -procedure. It is proved that the analysis strategy in [7] is more relaxed, because it removes a limitation that exists within the analysis framework based on **the convex hull representation method**, this limitation requires the level set of the Lyapunov function to be contained within the polyhedron  $L(\mathbf{H}) = \mathbf{x} : |\mathbf{H}\mathbf{x}|_\infty \leq 1$ , where  $\mathbf{H}$  is the auxiliary controller gain. Although the analysis strategy in [7] effectively reduces the conservatism of the analysis results and expands the estimation of DOA, the nonconvex problem of the resultant conditions remains unsolved, so the controller gains and the decision variables  $\tau_j$  need to be obtained by a complex iterative algorithm, which motivates us to focus on the de-convexification of the resultant conditions.

In addition to the handling method of the saturation function, the shape of the level set of Lyapunov function also affects the conservatism of the DOA estimation. It has been proved that the level set of the linear copositive Lyapunov function can provide relaxed estimation of DOA [29], but when it is used to estimate the DOA of the continuous-time positive fuzzy systems with input saturation [30], the non-convex problem caused by membership functions is a big challenge, especially when the IPM controller design strategy is adopted. Although the convexification method in [31] can handle the non-convex terms formed by the coupling of the controller gains and the Lyapunov variables, the non-convex terms formed by the coupling of the function variables themselves still cannot be handled. Also, the **membership-function-dependent (MFD)** method of the convexification method in [31] is still conservative, because the piecewise linear membership function approximation method has limited ability to approximate the initial membership function. In the existing **literature**, the Taylor-series membership function [32, 33] and polynomial membership function [34, 35] provide higher approximation ability by increasing the order of the polynomial terms, which inevitably increases the computational burden and even the Runge phenomenon may appear. Although the Chebyshev membership function in [36] avoids Runge phenomenon, it did not consider the influence of the shape characteristics of the membership function on approximation errors. Thus, it will become the focus of this paper to reduce the conservatism of the MFD method without increasing the computational burden.

In this paper, the estimation of DOA is investigated for continuous-time positive polynomial fuzzy systems with input saturation, and the fuzzy controller is designed based on IPM controller design strategy. With the goal of expanding the estimation of DOA, a less conservative analysis strategy is implemented, and corresponding countermeasures are proposed for the challenges encountered in the implementation of the analysis strategy. The **detailed** innovations and contributions of this paper are summarized below:

- 1) The DOA estimation of continuous-time positive polynomial fuzzy systems subject to input saturation is investigated under the IPM controller design strategy, where the saturation function is expressed as an inequality form, also the DOA constraint condition is embedded into the stability conditions and positivity conditions without introducing the decision variable. The above analysis strategy will prove to be less conservative.
- 2) Two novel inequality lemmas are provided to handle the non-convex term derived from the above analysis framework, also the **MFD method is utilized** to handle the non-convex term caused by the unmatched premise membership functions, so that some convex resultant conditions are obtained to avoid the use of complex iterative algorithms when solving controller gains.
- 3) A novel Chebyshev approximation algorithm is proposed to obtain a less conservative MFD method which can be used to handle the non-convex term and relax the resultant conditions. In this approximation algorithm, the state space is divided by the breakpoints of the first-order derivative of the membership function, and the order of the approximated membership function is chosen based on the maximum curvature of **the state subspace**, so this novel Chebyshev approximation algorithm has the ability to improve the approximation errors without increasing the computational burden, especially for non-smooth membership functions.

## 99 2. PRELIMINARY

### 100 2.1. Notation

101 The following notation will be adopted throughout this article.  $\mathfrak{Z} > 0$  (or  $\mathfrak{Z} < 0$ ) means that all elements of  $\mathfrak{Z}$  are  
 102 positive (or negative), and  $\mathfrak{Z} \geq 0$  (or  $\mathfrak{Z} \leq 0$ ) means that  $\mathfrak{Z}$  is **positive semi-definite** (or negative semi-definite).  $\mathfrak{Z}^{(\alpha,\beta)}$   
 103 is the  $\alpha^{\text{th}}$  row,  $\beta^{\text{th}}$  column element of  $\mathfrak{Z}$ .  $\mathfrak{R}^{n \times m}$  represents an  $n \times m$  dimensional matrix over the real number field.  $\mathfrak{C}$   
 104 is called a **Metzler matrix** if its **off-diagonal** elements are all nonnegative [4].  $\underline{n}$  represents  $1, 2, \dots, n$ . A polynomial  $h(\mathbf{x}(t))$   
 105 is an **Sum-of-Squares (SOS)** if **there exist polynomials**  $h_1(\mathbf{x}(t)), h_2(\mathbf{x}(t)), \dots, h_c(\mathbf{x}(t))$  such that  $h(\mathbf{x}(t)) = \sum_{i=1}^c h_i^2(\mathbf{x}(t))$ ,  
 106 where  $h_i(\mathbf{x}(t))$  is a polynomial and  $c$  is a positive integer, so  $h(\mathbf{x}(t))$  being an SOS naturally implies  $h(\mathbf{x}(t)) \geq 0$  for all  
 107  $\mathbf{x}(t)$ .

108 **Lemma 1.** [37] *The following inequality holds true for a scalar  $\gamma$  and symmetric matrices  $\mathbf{K}$  and  $\mathbf{S}$  with suitable*  
 109 *dimensions,  $\mathbf{S} > 0$ :*

$$-\mathbf{K}\mathbf{S}^{-1}\mathbf{K} \leq \gamma^2\mathbf{S} - 2\gamma\mathbf{K}.$$

### 110 2.2. Polynomial Fuzzy Plant Model with Input Saturation

111 In this paper, the polynomial fuzzy modeling approach is employed to model a nonlinear positive system with input  
 112 saturation constraints as a polynomial fuzzy positive system with  $p$  fuzzy rules. The  $i$ -th rule is as follows:

$$\begin{aligned} \text{Rule } i : & \text{ IF } f_1(\mathbf{x}(t)) \text{ is } M_1^i \text{ AND } \dots \text{ AND } f_\psi(\mathbf{x}(t)) \text{ is } M_\psi^i, \\ & \text{ THEN } \dot{\mathbf{x}}(t) = \mathbf{A}_i(\mathbf{x}(t))\mathbf{x}(t) + \mathbf{B}_i(\mathbf{x}(t))\text{sat}(\mathbf{u}(t)) \end{aligned}$$

113 where  $f_g(\mathbf{x}(t))$  is the premise variable and  $M_g^i$  is the fuzzy set corresponding to premise variable  $f_g(\mathbf{x}(t))$  in rule  $i$   
 114 ,  $i \in p, g \in \psi$ , and  $\psi$  is a positive integer;  $\mathbf{x}(t) \in \mathfrak{R}^n$  and  $\mathbf{u}(t) \in \mathfrak{R}^m$  are the state vector and control input vector  
 115 of the system, respectively;  $\mathbf{A}_i(\mathbf{x}(t)) \in \mathfrak{R}^{n \times n}$ ,  $\mathbf{B}_i(\mathbf{x}(t)) \in \mathfrak{R}^{n \times m}$  are the known polynomial system matrices and input  
 116 matrices, respectively.  $n, m$  are their dimensions. The function  $\text{sat}(\cdot) : \mathfrak{R}^m \rightarrow \mathfrak{R}^m$  is a standard saturation function  
 117 defined as:

$$\text{sat}(\mathbf{u}(t)) = [\text{sat}(\mathbf{u}^{(1)}(t)), \text{sat}(\mathbf{u}^{(2)}(t)), \dots, \text{sat}(\mathbf{u}^{(m)}(t))]^T \quad (1)$$

118 where

$$\text{sat}(\mathbf{u}^{(i)}(t)) = \begin{cases} u_{lim} & \text{if } \mathbf{u}^{(i)}(t) > u_{lim} \\ \mathbf{u}^{(i)}(t) & \text{if } -u_{lim} \leq \mathbf{u}^{(i)}(t) \leq u_{lim}, \\ -u_{lim} & \text{if } \mathbf{u}^{(i)}(t) < -u_{lim} \end{cases}$$

119  $\mathbf{u}^{(i)}(t)$  is the  $i^{\text{th}}$  element of  $\mathbf{u}(t)$ ,  $u_{lim}$  is the control input limit.

120 Based on the fuzzy rules mentioned above, when fuzzification, fuzzy inference, and defuzzification being applied  
 121 to the nonlinear system, the entire nonlinear system can be formulated as the following polynomial fuzzy system:

$$\dot{\mathbf{x}} = \sum_{i=1}^p w_i(\mathbf{x}(t))(\mathbf{A}_i(\mathbf{x}(t))\mathbf{x}(t) + \mathbf{B}_i(\mathbf{x}(t))\text{sat}(\mathbf{u}(t))) \quad (2)$$

122 where  $w_i(\mathbf{x}(t))$  is the normalized grade of membership,  $w_i(\mathbf{x}(t)) \geq 0$ , and  $\sum_{i=1}^p w_i(\mathbf{x}(t)) = 1$ .

### 123 2.3. Polynomial Fuzzy Controller

124 This paper designs a polynomial fuzzy controller based on the IPM concept **\*\*and\*\*** follows a similar modeling  
 125 procedure to that in reference [33]; the designed polynomial fuzzy controller is represented by the following equation:

$$\mathbf{u}(t) = \sum_{j=1}^p m_j(\mathbf{x}(t))\mathbf{G}_j(\mathbf{x}(t))\mathbf{x}(t), \quad (3)$$

126 where  $m_j(\mathbf{x}(t))$  is a membership function distinct from the system's membership function  $w_i(\mathbf{x}(t))$ , satisfying  $m_j(\mathbf{x}(t)) \geq$   
 127  $0$  and  $\sum_{j=1}^p m_j(\mathbf{x}(t)) = 1$ . and  $\mathbf{G}_j(\mathbf{x}(t))$  is the gain of the polynomial fuzzy controller to be designed.

## 2.4. Saturated Input Control

The saturation function is a type of nonlinear function. To remove the obstacles of nonlinear characteristics to system analysis, the saturation function can be represented by the following crucial inequality [7]:

$$\begin{cases} \text{sat}(\mathbf{u}^{(k,\cdot)}(t)) \geq \min\{u_{lim}, \sum_{j=1}^c m_j(\mathbf{x})\mathbf{G}_j^{(k,\cdot)}(\mathbf{x}(t))\mathbf{x}(t)\} \\ \text{sat}(\mathbf{u}^{(k,\cdot)}(t)) \leq \max\{-u_{lim}, \sum_{j=1}^c m_j(\mathbf{x})\mathbf{G}_j^{(k,\cdot)}(\mathbf{x}(t))\mathbf{x}(t)\} \end{cases} \quad (4)$$

**Remark 1.** The nonlinear saturation function  $\text{sat}(\mathbf{u}(t))$  is represented by its upper and lower bounds in (4). *\*\*These\*\** upper and lower bounds are used to perform stability and positivity analysis for the saturated positive polynomial fuzzy system (2), respectively. The representation (4) of the saturation function fits well with the analytical characteristics of positive systems. Furthermore, compared with the convex hull representation, it does not require the introduction of auxiliary controllers for assisting analysis.

For simplicity, the time symbol 't' will be omitted in the subsequent analysis in this paper.

## 3. MAIN RESULTS

The objective of this paper is to design a polynomial fuzzy controller to make closed-loop system (2) positive and asymptotically stable over the largest possible DOA, and the following theorem is proposed to design the polynomial fuzzy controller gains.

**Theorem 1.** The saturated polynomial fuzzy system (2) is asymptotically stable and remains non-negative in a maximum DOA if there exist vectors  $\lambda \in \mathfrak{R}^n$ , scalars  $\tilde{\lambda}$  and  $\check{\lambda}$ , polynomial matrices  $\tilde{\mathbf{L}}_{jl}(\mathbf{x}) \in \mathfrak{R}^{1 \times n}$  and  $\mathbf{O}_j(\mathbf{x}) \in \mathfrak{R}^{m \times n}$ , and positive polynomial scalars  $Y_{q_1 i}(\mathbf{x})$ ,  $Y_{q_2 s}(\mathbf{x})$  and  $R_{\hat{q}\zeta^*}(\mathbf{x})$ ,  $\forall q_1 \in \{1, 2\}$ ,  $q_2 \in \{3, 4\}$ ,  $\hat{q} \in \{1, 2, 3\}$ ,  $i, s \in \underline{p}$ ,  $\zeta^* \in \underline{\sigma^*}$ , such that the following SOS-based conditions are satisfied:

$$\begin{aligned} & \min \hat{\ell} \\ & \text{s.t. a) } v^T(\hat{\ell} - \lambda^T \mathbf{x}_0^T)v \text{ is SOS;} \\ & \quad \text{b) } v^T(\lambda^{(\alpha)} - \vartheta_1)v \text{ is SOS; } \forall \alpha \in \underline{n} \\ & \quad \text{c) } v^T[\tilde{\mathbf{L}}_{jl}^{(\beta)}(\mathbf{x}) - (\mathbf{D}_l^- \mathbf{O}_j(\mathbf{x}))^{(r,\beta)}(\mathbf{x})]v \text{ is SOS; } \forall j \in \underline{p}, l \in \underline{2^m}, \beta \in \underline{n}, r \in \underline{m} \\ & \quad \text{d) } v^T(\lambda^T \mathbf{x} - \tilde{\lambda} \mathbf{e}_n^T \mathbf{x})v \text{ is SOS;} \\ & \quad \text{e) } v^T(\lambda^T \mathbf{B}_i(\mathbf{x})\mathbf{D}_l \mathbf{e}_m - \tilde{\lambda} \mathbf{e}_n^T \mathbf{B}_i(\mathbf{x})\mathbf{D}_l \mathbf{e}_m)v \text{ is SOS; } \forall i \in \underline{p}, l \in \underline{2^m} \\ & \quad \text{f) } v^T(Y_{q_1 i}(\mathbf{x}) - \vartheta_2(\mathbf{x}))v \text{ is SOS; } \forall q_1 \in \{1, 2\}, i \in \underline{p} \\ & \quad \text{g) } v^T(Y_{q_2 s}(\mathbf{x}) - \vartheta_3(\mathbf{x}))v \text{ is SOS; } \forall q_2 \in \{3, 4\}, s \in \underline{p} \\ & \quad \text{h) } v^T(Y_{q_1 i}(\mathbf{x}) - \varpi_i(\mathbf{x}) - \vartheta_4(\mathbf{x}))v \text{ is SOS; } \forall q_1 \in \{1, 2\}, i \in \underline{p} \\ & \quad \text{i) } v^T(Y_{q_2 s}(\mathbf{x}) - \varpi_s(\mathbf{x}) - \vartheta_5(\mathbf{x}))v \text{ is SOS; } \forall q_2 \in \{3, 4\}, s \in \underline{p} \\ & \quad \text{j) } v^T(R_{\hat{q}\zeta^*}(\mathbf{x}) - \vartheta_6(\mathbf{x}))v \text{ is SOS; } \forall \hat{q} \in \{1, 2, 3\}, \zeta^* \in \underline{\sigma^*} \\ & \quad \text{k) } v^T(\Xi_{1\zeta^*}(\mathbf{x}) - \vartheta_7(\mathbf{x}))v \text{ is SOS; } \forall \zeta^* \in \underline{\sigma^*} \\ & \quad \text{l) } v^T\Xi_{2\zeta^*}(\mathbf{x})v \text{ is SOS; } \forall \zeta^* \in \underline{\sigma^*} \\ & \quad \text{m) } v^T\Xi_{3\zeta^*}(\mathbf{x})v \text{ is SOS; } \forall \zeta^* \in \underline{\sigma^*} \\ & \quad \text{n) } -v^T(\Upsilon_{ijl1}^{(\alpha)}(\mathbf{x}) - \vartheta_8(\mathbf{x}))v \text{ is SOS; } \forall i, j \in \underline{p}, l \in \underline{2^m}, \alpha \in \underline{n} \\ & \quad \text{o) } -v^T(\Upsilon_{ijl2}^{(\alpha)}(\mathbf{x}) - \vartheta_9(\mathbf{x}))v \text{ is SOS; } \forall i, j \in \underline{p}, l \in \underline{2^m}, \alpha \in \underline{n} \\ & \quad \text{p) } v^T(\lambda^T \mathbf{B}_s(\mathbf{x})\mathbf{e}_m - \check{\lambda} \mathbf{e}_n^T \mathbf{B}_s(\mathbf{x})\mathbf{e}_m)v \text{ is SOS; } \forall s \in \underline{p} \\ & \quad \text{q) } v^T[\sum_{\beta: \beta \neq \alpha \in \underline{n}} (\mathbf{B}_i(\mathbf{x})\mathbf{D}_l \mathbf{e}_m)^{(\alpha,\cdot)}(\lambda^T)^{(\cdot,\beta)} \mathbf{x}^{(\beta)} - \sum_{\beta: \beta \neq \alpha \in \underline{n}} (\mathbf{B}_i(\mathbf{x})\mathbf{D}_l \mathbf{e}_m)^{(\alpha,\cdot)} \check{\lambda} \mathbf{x}^{(\beta)}]v \text{ is SOS; } \forall i \in \underline{p}, l \in \underline{2^m}, \alpha, \beta \in \underline{n} \\ & \quad \text{r) } v^T(\Theta_{ijst}^{(\alpha,\beta)}(\mathbf{x}) - \vartheta_{10}(\mathbf{x}))v \text{ is SOS; } \forall i, j, s \in \underline{p}, l \in \underline{2^m}, \alpha, \beta \in \underline{n}, \alpha \neq \beta \end{aligned} \quad (5)$$

145 The description of  $\Xi_{1\zeta^*}(\mathbf{x})$ ,  $\Xi_{2\zeta^*}(\mathbf{x})$ ,  $\Xi_{3\zeta^*}(\mathbf{x})$ ,  $\Upsilon_{ijl1}(\mathbf{x})$ ,  $\Upsilon_{ijl2}(\mathbf{x})$  and  $\Theta_{ijsl}^{(\alpha,\beta)}(\mathbf{x})$  can be found in (35), (36), (37), (18), (19)  
 146 and (44), respectively. The polynomial fuzzy controller gain is represented by  $\mathbf{G}_j(\mathbf{x}) = \frac{\mathbf{O}_j(\mathbf{x})}{\sum_{s=1}^p \lambda^T \mathbf{B}_s(\mathbf{x}) \mathbf{e}_m}$  which is obtained  
 147 by solving the aforementioned SOS conditions.

148 **Remark 2.** It is necessary to introduce the main parameters that appear in it:  $\hat{\ell}$  is the optimization parameter for the  
 149 DOA;  $\lambda$  is the Lyapunov function variable;  $\mathbf{v}$  is any vector of arbitrary dimension, independent of  $\mathbf{x}$ ;  $\vartheta_1 - \vartheta_{10}(\mathbf{x})$  are  
 150 predefined positive scalar polynomials;  $\gamma_1$  and  $\gamma_2$  are parameters introduced by Lemma 1;  $\tilde{\lambda}$  is a parameter introduced  
 151 by Lemma 2;  $\check{\lambda}$  is a parameter introduced utilizing Lemma 3 and finally,  $\sigma^*$  denotes the number of subspaces into which  
 152 the state space is partitioned for the purposes of the Chebyshev piecewise approximation.

153 **Proof 1.** This proof consists of three parts: stability analysis, positive analysis, and maximization of DOA. In the  
 154 stability analysis part, a novel analysis method is proposed which incorporates the conditions of the estimation of  
 155 DOA. The nonconvex terms of the analysis resultant conditions are effectively handled by the novel convexification  
 156 methods, and the nonconvex positivity analysis resultant conditions are handled by the inequality lemma proposed in  
 157 this paper.

### 158 Part I: Stability Analysis

159 In order to perform the stability analysis for the saturated positive polynomial fuzzy system (2), the following linear  
 160 copositive Lyapunov function is adopted:

$$\mathbf{V}(\mathbf{x}) = \lambda^T \mathbf{x} \quad (6)$$

161 Combining equation (4), the following inequality can be obtained.

$$\begin{aligned} \dot{\mathbf{V}}(\mathbf{x}) &= \sum_{i=1}^p w_i(\mathbf{x}) \lambda^T (\mathbf{A}_i(\mathbf{x})\mathbf{x} + \mathbf{B}_i(\mathbf{x})\text{sat}(\mathbf{u})) \\ &\leq \sum_{i=1}^p w_i(\mathbf{x}) \lambda^T \mathbf{A}_i(\mathbf{x})\mathbf{x} + \sum_{i=1}^p w_i(\mathbf{x}) \lambda^T \times \sum_{k=1}^m \mathbf{B}_i^{(:,k)}(\mathbf{x}) \max\{-u_{lim}, \sum_{j=1}^p m_j(\mathbf{x}) \mathbf{G}_j^{(k,\cdot)}(\mathbf{x})\mathbf{x}\} \\ &= \sum_{i=1}^p w_i(\mathbf{x}) \lambda^T \mathbf{A}_i(\mathbf{x})\mathbf{x} + \max_{1 \leq l \leq 2^m} \left\{ \sum_{i=1}^p \sum_{j=1}^p w_i(\mathbf{x}) m_j(\mathbf{x}) [-u_{lim} \lambda^T \mathbf{B}_i(\mathbf{x}) \mathbf{D}_l \mathbf{e}_m + \lambda^T \mathbf{B}_i(\mathbf{x}) \mathbf{D}_l^- \mathbf{G}_j(\mathbf{x})\mathbf{x}] \right\} \end{aligned} \quad (7)$$

162 where  $\mathbf{e}_m \in \mathfrak{R}^{m \times 1}$  is a column vector with all elements being 1;  $\mathbf{D}_l$  is a diagonal matrix with diagonal elements of 0  
 163 or 1,  $\forall l \in \underline{2^m}$ .

164 It should be noted that the saturated system is not globally stable but only locally stable, which should be taken  
 165 into account in the stability analysis. In this paper, this local region is estimated by the level set of the linear copositive  
 166 Lyapunov function as follows:

$$\mathbf{P}(\lambda) := \{\mathbf{x} \geq 0, \lambda^T \mathbf{x} \leq 1\} \quad (8)$$

167 By introducing the level set inequality condition (8) into (7), the following inequality can be obtained:

$$\dot{\mathbf{V}}(\mathbf{x}) \leq \max_{1 \leq l \leq 2^m} \sum_{i=1}^p \sum_{j=1}^p w_i(\mathbf{x}) m_j(\mathbf{x}) [\lambda^T \mathbf{A}_i(\mathbf{x})\mathbf{x} - u_{lim} \lambda^T \mathbf{B}_i(\mathbf{x}) \mathbf{D}_l \mathbf{e}_m \lambda^T \mathbf{x} + \lambda^T \mathbf{B}_i(\mathbf{x}) \mathbf{D}_l^- \mathbf{G}_j(\mathbf{x})\mathbf{x}] \quad (9)$$

168 Inequality (9) still contains two non-convex terms,  $-u_{lim} \lambda^T \mathbf{B}_i(\mathbf{x}) \mathbf{D}_l \mathbf{e}_m \lambda^T \mathbf{x}$  and  $\lambda^T \mathbf{B}_i(\mathbf{x}) \mathbf{D}_l^- \mathbf{G}_j(\mathbf{x})\mathbf{x}$ . Next, these two  
 169 non-convex terms will be individually convexified.

170 **A : The convexification of the non-convex term  $-u_{lim}\lambda^T \mathbf{B}_i(\mathbf{x})\mathbf{D}_l\mathbf{e}_m\lambda^T \mathbf{x}$**

171 **Lemma 2.** There always exists a parameter  $\tilde{\lambda}$  such that the following inequations hold:

$$\lambda^T \mathbf{x} \geq \tilde{\lambda} \mathbf{e}_n^T \mathbf{x}, \quad (10)$$

$$\lambda^T \mathbf{B}_i(\mathbf{x})\mathbf{D}_l\mathbf{e}_m \geq \tilde{\lambda} \mathbf{e}_n^T \mathbf{B}_i(\mathbf{x})\mathbf{D}_l\mathbf{e}_m, \quad (11)$$

172 where  $\tilde{\lambda}$  is undecided scalar.  $\mathbf{e}_m \in \mathfrak{R}^{m \times 1}$  is a column vector with all elements being 1, and  $\mathbf{e}_n \in \mathfrak{R}^{n \times 1}$  is similar to  $\mathbf{e}_m$ .

173 The Lemma 2 is utilized to handle the non-convex term  $-u_{lim}\lambda^T \mathbf{B}_i(\mathbf{x})\mathbf{D}_l\mathbf{e}_m\lambda^T \mathbf{x}$ , then (9) can be derived as follows:

$$\dot{\mathbf{V}}(\mathbf{x}) \leq \max_{1 \leq l \leq 2^m} \left\{ \sum_{i=1}^p \sum_{j=1}^p w_i(\mathbf{x})m_j(\mathbf{x}) \left[ \lambda^T \mathbf{A}_i(\mathbf{x}) - u_{lim} \tilde{\lambda} \mathbf{e}_n^T \mathbf{B}_i(\mathbf{x})\mathbf{D}_l\mathbf{e}_m \tilde{\lambda} \mathbf{e}_n^T + \lambda^T \mathbf{B}_i(\mathbf{x})\mathbf{D}_l^- \mathbf{G}_j(\mathbf{x}) \right] \mathbf{x} \right\} \quad (12)$$

174 According to the Lemma 1, the following inequation holds:

$$-u_{lim} \tilde{\lambda} \mathbf{e}_n^T \mathbf{B}_i(\mathbf{x})\mathbf{D}_l\mathbf{e}_m \tilde{\lambda} \leq u_{lim} \mathbf{e}_n^T \mathbf{B}_i(\mathbf{x})\mathbf{D}_l\mathbf{e}_m (\gamma_1^2 - 2\gamma_1 \tilde{\lambda}) \quad (13)$$

175 Then, the following inequation holds:

$$\dot{\mathbf{V}}(\mathbf{x}) \leq \max_{1 \leq l \leq 2^m} \left\{ \sum_{i=1}^p \sum_{j=1}^p w_i(\mathbf{x})m_j(\mathbf{x}) \left[ \lambda^T \mathbf{A}_i(\mathbf{x}) + u_{lim} \mathbf{e}_n^T \mathbf{B}_i(\mathbf{x})\mathbf{D}_l\mathbf{e}_m (\gamma_1^2 - 2\gamma_1 \tilde{\lambda}) \mathbf{e}_n^T + \lambda^T \mathbf{B}_i(\mathbf{x})\mathbf{D}_l^- \mathbf{G}_j(\mathbf{x}) \right] \mathbf{x} \right\} \quad (14)$$

176 **B : The convexification of the non-convex term  $\lambda^T \mathbf{B}_i(\mathbf{x})\mathbf{D}_l^- \mathbf{G}_j(\mathbf{x})$**

177 For the non-convex term  $\lambda^T \mathbf{B}_i(\mathbf{x})\mathbf{D}_l^- \mathbf{G}_j(\mathbf{x})$ , the controller gain is designed as  $\mathbf{G}_j(\mathbf{x}) = \frac{\mathbf{O}_j(\mathbf{x})}{\sum_{s=1}^p \lambda^T \mathbf{B}_s(\mathbf{x})\mathbf{e}_m} \in \mathfrak{R}^{m \times n}$ ,

178 where  $\mathbf{e}_m \in \mathfrak{R}^{m \times 1}$  is a column vector with all elements being 1,  $\mathbf{e}_m^k$  denotes only the  $k^{\text{th}}$  element of  $\mathbf{e}_m$  is 1, other elements are 0.  $\lambda$  is the undecided variable of the linear copositive Lyapunov function.

180 Let  $\mathbf{Q}_{jl}(\mathbf{x}) = \mathbf{D}_l^- \mathbf{O}_j(\mathbf{x})$ , if there exists a polynomial variable  $\tilde{\mathbf{L}}_{jl}(\mathbf{x}) \in \mathfrak{R}^{1 \times n}$  that satisfies  $\tilde{\mathbf{L}}_{jl}(\mathbf{x}) \geq \mathbf{Q}_{jl}^{(r,:)}(\mathbf{x})$  (where  
181  $\mathbf{Q}_{jl}^{(r,:)}(\mathbf{x})$  denotes the  $r$ -th row vector of  $\mathbf{Q}_{jl}(\mathbf{x})$ ), which means that the  $\beta$ -th element of  $\mathbf{Q}_{jl}^{(r,:)}(\mathbf{x})$  is less than or equal to  
182 the  $\beta$ -th element of  $\tilde{\mathbf{L}}_{jl}(\mathbf{x})$  for all  $\beta \in \underline{n}$  and  $r \in \underline{m}$ , then (14) can be derived as follows:

$$\begin{aligned} \dot{\mathbf{V}}(\mathbf{x}) &\leq \max_{1 \leq l \leq 2^m} \left\{ \sum_{i=1}^p \sum_{j=1}^p w_i(\mathbf{x})m_j(\mathbf{x}) \left[ \lambda^T \mathbf{A}_i(\mathbf{x}) + u_{lim} \mathbf{e}_n^T \mathbf{B}_i(\mathbf{x})\mathbf{D}_l\mathbf{e}_m (\gamma_1^2 - 2\gamma_1 \tilde{\lambda}) \mathbf{e}_n^T + \lambda^T \mathbf{B}_i(\mathbf{x}) \times \right. \right. \\ &\quad \left. \frac{\mathbf{D}_l^- \mathbf{O}_j(\mathbf{x})}{\sum_{s=1}^p m_s(\mathbf{x}) \lambda^T \mathbf{B}_s(\mathbf{x})\mathbf{e}_m} \right] \mathbf{x} \right\}. \\ &\leq \max_{1 \leq l \leq 2^m} \left\{ \sum_{i=1}^p w_i(\mathbf{x}) \left[ \lambda^T \mathbf{A}_i(\mathbf{x}) \mathbf{x} + u_{lim} \mathbf{e}_n^T \mathbf{B}_i(\mathbf{x})\mathbf{D}_l\mathbf{e}_m (\gamma_1^2 - 2\gamma_1 \tilde{\lambda}) \mathbf{x} \right] + \frac{\sum_{i=1}^p w_i(\mathbf{x}) \lambda^T \mathbf{B}_i(\mathbf{x})\mathbf{e}_m}{\sum_{s=1}^p m_s(\mathbf{x}) \lambda^T \mathbf{B}_s(\mathbf{x})\mathbf{e}_m} \times \right. \\ &\quad \left. \sum_{j=1}^p m_j(\mathbf{x}) \tilde{\mathbf{L}}_{jl}(\mathbf{x}) \mathbf{x} \right\}. \end{aligned} \quad (15)$$

183 For the non-convex term  $f(\mathbf{x}) := \frac{\sum_{i=1}^p w_i(\mathbf{x}) \lambda^T \mathbf{B}_i(\mathbf{x})\mathbf{e}_m}{\sum_{s=1}^p m_s(\mathbf{x}) \lambda^T \mathbf{B}_s(\mathbf{x})\mathbf{e}_m}$  in (15), the sector nonlinearity technique is adopted to fuzzify

184 it. Assume that positive scalars  $f_{min}$  and  $f_{max}$  are the minimum and maximum values of  $\frac{\sum_{i=1}^p w_i(\mathbf{x}) \lambda^T \mathbf{B}_i(\mathbf{x})\mathbf{e}_m}{\sum_{s=1}^p m_s(\mathbf{x}) \lambda^T \mathbf{B}_s(\mathbf{x})\mathbf{e}_m}$  in the  
185 operating domain of  $\mathbf{x}$  defined previously, respectively. Then the nonlinear term  $f(\mathbf{x})$  is represented as follows:

$$f(\mathbf{x}) = \mu_{\mathbf{M}^1}(\mathbf{x})f_{min} + \mu_{\mathbf{M}^2}(\mathbf{x})f_{max}, \quad (16)$$

186 where  $\mu_{M^1}(\mathbf{x}) = \frac{f(\mathbf{x}) - f_{\max}}{f_{\min} - f_{\max}}$ ,  $\mu_{M^2}(\mathbf{x}) = 1 - \mu_{M^1}(\mathbf{x})$ .  $f_{\max}$  and  $f_{\min}$  are two constants that are slightly greater than and  
 187 less than 1 respectively in a case that  $w_i(\mathbf{x})$  and  $m_i(\mathbf{x})$  are closed to each other.

188 After the above treatment of non-convex terms and defining  $f_1 = f_{\min}$ ,  $f_2 = f_{\max}$ , equation (15) can be represented  
 189 as follows:

$$\begin{aligned} \dot{\mathbf{V}}(\mathbf{x}) &< \max_{1 \leq l \leq 2^m} \left\{ \sum_{i=1}^p w_i(\mathbf{x}) [\lambda^T \mathbf{A}_i(\mathbf{x}) \mathbf{x} + u_{lim} \mathbf{e}_n^T \mathbf{B}_i(\mathbf{x}) \mathbf{D}_l \mathbf{e}_m (\gamma_1^2 - 2\gamma_1 \tilde{\lambda}) \mathbf{x}] + \sum_{j=1}^p \sum_{v=1}^2 m_j(\mathbf{x}) \mu_{M^v} f_v \tilde{\mathbf{L}}_{jl}(\mathbf{x}) \mathbf{x} \right\} \\ &= \max_{1 \leq l \leq 2^m} \left\{ \sum_{i=1}^p \sum_{j=1}^p \sum_{v=1}^2 w_i(\mathbf{x}) m_j(\mathbf{x}) \mu_{M^v} [\lambda^T \mathbf{A}_i(\mathbf{x}) + u_{lim} \mathbf{e}_n^T \mathbf{B}_i(\mathbf{x}) \mathbf{D}_l \mathbf{e}_m (\gamma_1^2 - 2\gamma_1 \tilde{\lambda}) \mathbf{e}_n^T + f_v \tilde{\mathbf{L}}_{jl}(\mathbf{x})] \mathbf{x} \right\}. \end{aligned} \quad (17)$$

190 The following definitions are given:

$$\mathbf{Y}_{ijl1}(\mathbf{x}) = \lambda^T \mathbf{A}_i(\mathbf{x}) + u_{lim} \mathbf{e}_n^T \mathbf{B}_i(\mathbf{x}) \mathbf{D}_l \mathbf{e}_m (\gamma_1^2 - 2\gamma_1 \tilde{\lambda}) \mathbf{e}_n^T + f_1 \tilde{\mathbf{L}}_{jl}(\mathbf{x}) \quad (18)$$

$$\mathbf{Y}_{ijl2}(\mathbf{x}) = \lambda^T \mathbf{A}_i(\mathbf{x}) + u_{lim} \mathbf{e}_n^T \mathbf{B}_i(\mathbf{x}) \mathbf{D}_l \mathbf{e}_m (\gamma_1^2 - 2\gamma_1 \tilde{\lambda}) \mathbf{e}_n^T + f_2 \tilde{\mathbf{L}}_{jl}(\mathbf{x}) \quad (19)$$

191 Due to the conditions  $0 \leq \mu_{M^1}(\mathbf{x}) \leq 1$ , and  $0 \leq \mu_{M^2}(\mathbf{x}) \leq 1$ , also all elements of the system state  $\mathbf{x}$  are non-negative  
 192 for positive system, if the following conditions hold, it can be concluded that  $\dot{\mathbf{V}}(\mathbf{x}) < 0$  is satisfied:

$$\sum_{i=1}^p \sum_{j=1}^p w_i(\mathbf{x}) m_j(\mathbf{x}) \mathbf{Y}_{ijl1}(\mathbf{x}) < 0 \quad (20)$$

$$\sum_{i=1}^p \sum_{j=1}^p w_i(\mathbf{x}) m_j(\mathbf{x}) \mathbf{Y}_{ijl2}(\mathbf{x}) < 0 \quad (21)$$

$$f_{\min} \leq \frac{\sum_{i=1}^p w_i(\mathbf{x}) \lambda^T \mathbf{B}_i(\mathbf{x}) \mathbf{e}_m}{\sum_{s=1}^p m_s(\mathbf{x}) \lambda^T \mathbf{B}_s(\mathbf{x}) \mathbf{e}_m} \leq f_{\max} \quad (22)$$

193 It should be noted that the polynomial resultant conditions need to be calculated by SOSTOOLS toolbox to obtain  
 194 the controller gains, but **this toolbox cannot handle nonlinear terms, such as nonlinear membership functions**. For  
 195 conditions (20) and (21), they are guaranteed by  $\mathbf{Y}_{ijl1}(\mathbf{x}) < 0$  and  $\mathbf{Y}_{ijl2}(\mathbf{x}) < 0$  **if the membership functions  $w_i(\mathbf{x})$  and**  
 196  **$m_j(\mathbf{x})$  are both greater than zero**. However, the nonlinear membership functions embedded in condition (22) cannot  
 197 be ignored. To handle the nonconvex condition (22), an advanced Chebyshev approximation method is proposed to  
 198 perform piecewise approximation for the initial nonlinear membership function. **The obtained piecewise Chebyshev**  
 199 **membership function is described in polynomial form, so it can be calculated by the SOSTOOLS toolbox**.

200 To be specific, the nonlinear membership functions  $w_i(\mathbf{x})$  and  $m_s(\mathbf{x})$  are approximated by the following piecewise  
 201 Chebyshev membership function:

$$w_i(\mathbf{x}) = \sum_{\zeta^*=1}^{\sigma^*} \varphi_{\zeta^*}(\mathbf{x}) \left( a_{0i\zeta^*}^* + \sum_{q_w=1}^{\kappa_{w\zeta^*}^*} a_{q_w i \zeta^*}^* \chi_{q_w}(\mathbf{x}) \right), \quad (23)$$

$$m_s(\mathbf{x}) = \sum_{\zeta^*=1}^{\sigma^*} \varphi_{\zeta^*}(\mathbf{x}) \left( b_{0s\zeta^*}^* + \sum_{q_m=1}^{\kappa_{m\zeta^*}^*} b_{q_m s \zeta^*}^* \varrho_{q_m}(\mathbf{x}) \right), \quad (24)$$

202 where  $\sigma^*$  is the number into which the state space is divided when the membership function is approximated piecewise,  
 203 and each state subspace is denoted as  $\Psi_{\zeta^*}, \zeta^* \in \underline{\sigma^*}$ . When  $\mathbf{x} \in \Psi_{\zeta^*}$ ,  $\varphi_{\zeta^*}(\mathbf{x})$  is 1, and when  $\mathbf{x} \notin \Psi_{\zeta^*}$ ,  $\varphi_{\zeta^*}(\mathbf{x})$   
 204 is 0.  $\kappa_{w\zeta^*}^*$  and  $\kappa_{m\zeta^*}^*$  are the maximum approximate **orders** of  $w_i(\mathbf{x})$  and  $m_s(\mathbf{x})$  in state subspace  $\Psi_{\zeta^*}$ , respectively.  
 205  $\chi_{q_w}(\mathbf{x})$  and  $\varrho_{q_m}(\mathbf{x})$  are polynomials with order  $q_w$  and  $q_m$ , respectively. **The coefficients of these polynomials are**  
 206  **$a_{0i\zeta^*}^*, a_{1i\zeta^*}^*, \dots, a_{ni\zeta^*}^*$  and  $b_{0s\zeta^*}^*, b_{1s\zeta^*}^*, \dots, b_{ns\zeta^*}^*$ , which are optimized by the Remez algorithm**.

207 To obtain smaller approximate errors, the state space segmentation and approximation order selection of the  
 208 piecewise Chebyshev membership functions (23) and (24) are determined by Algorithm 1 in Appendix A.

209 **Remark 3.** In reference [36], the operating domain  $\Psi$  is equally divided into  $\sigma^*$  subspaces, it is suitable for smooth  
 210 membership functions, but it will lead to large approximation error for the non-smooth membership functions. In  
 211 addition, the maximum approximate order is the same in all subspace  $\Psi_{\zeta^*}$  in reference [36], i.e.,  $\kappa_{w_{\zeta^*}}$  is the same for  
 212 all subspace  $\Psi_{\zeta^*}$ , and  $\kappa_{m_{\zeta^*}}$  also is the same for all subspace  $\Psi_{\zeta^*}$ , which adds unnecessary computational burden and  
 213 **is not conducive** to reducing conservatism. In contrast, the state space segmentation  $\sigma^*$  and the maximum approximate  
 214 orders  $\kappa_{w_{\zeta^*}}$  and  $\kappa_{m_{\zeta^*}}$  in this paper are optimized by the Algorithm 1 proposed above, which measures the demand for  
 215 state space segmentation and approximate order according to the breakpoint of the first derivative of the membership  
 216 function and the curvature of the membership function, respectively. **This helps** to reduce the computational burden  
 217 and approximate error, and thus reduce the conservatism of the analysis results.

218 Denote the approximated sub-membership functions in state subspace  $\Psi_{\zeta^*}$  as  $\hat{w}_{i_{\zeta^*}}(\mathbf{x}) := a_{0i_{\zeta^*}}^* + \sum_{q_w=1}^{\kappa_{w_{\zeta^*}}} a_{q_w i_{\zeta^*}}^* \chi_{q_w}(\mathbf{x})$

219 and  $\hat{m}_{s_{\zeta^*}}(\mathbf{x}) := b_{0s_{\zeta^*}}^* + \sum_{q_m=1}^{\kappa_{m_{\zeta^*}}} b_{q_m s_{\zeta^*}}^* \rho_{q_m}(\mathbf{x})$ , the approximation errors of  $w_{i_{\zeta^*}}(\mathbf{x})$  and  $m_{s_{\zeta^*}}(\mathbf{x})$  are defined as  $\Delta w_{i_{\zeta^*}}(\mathbf{x}) =$   
 220  $w_{i_{\zeta^*}}(\mathbf{x}) - \hat{w}_{i_{\zeta^*}}(\mathbf{x})$  and  $\Delta m_{s_{\zeta^*}}(\mathbf{x}) = m_{s_{\zeta^*}}(\mathbf{x}) - \hat{m}_{s_{\zeta^*}}(\mathbf{x})$ , respectively. The upper boundary and lower boundary of  
 221  $\Delta w_{i_{\zeta^*}}(\mathbf{x})$  are  $\bar{\pi}_i$  and  $\underline{\pi}_i$ , respectively; the upper boundary and lower boundary of  $\Delta m_{s_{\zeta^*}}(\mathbf{x})$  are  $\bar{\phi}_s$  and  $\underline{\phi}_s$ , respectively.  
 222 These approximated membership functions and the approximation error can be used to replace the initial nonlinear  
 223 membership functions of condition (22). For simplicity, denote  $\varpi_i(\mathbf{x}) = \lambda^T \mathbf{B}_i(\mathbf{x}) \mathbf{e}_m$  and  $\varpi_s(\mathbf{x}) = \lambda^T \mathbf{B}_s(\mathbf{x}) \mathbf{e}_m$ , then the  
 224 terms that contain nonlinear membership functions in (22) can be handled as follows:

$$\underline{W}_{\varpi}(\mathbf{x}) \leq \sum_{i=1}^p w_i(\mathbf{x}) \varpi_i(\mathbf{x}) \leq \overline{W}_{\varpi}(\mathbf{x}) \quad (25)$$

$$\underline{M}_{\varpi}(\mathbf{x}) \leq \sum_{s=1}^p m_s(\mathbf{x}) \varpi_s(\mathbf{x}) \leq \overline{M}_{\varpi}(\mathbf{x}) \quad (26)$$

225 in which

$$\underline{W}_{\varpi}(\mathbf{x}) = \sum_{\zeta^*=1}^{\sigma^*} \varphi_{\zeta^*}(\mathbf{x}) \sum_{i=1}^p [(\hat{w}_{i_{\zeta^*}}(\mathbf{x}) + \bar{\pi}_{i_{\zeta^*}}) \varpi_i(\mathbf{x}) + (\underline{\pi}_{i_{\zeta^*}} - \bar{\pi}_{i_{\zeta^*}}) Y_{1i}(\mathbf{x})], \quad (27)$$

$$\overline{W}_{\varpi}(\mathbf{x}) = \sum_{\zeta^*=1}^{\sigma^*} \varphi_{\zeta^*}(\mathbf{x}) \sum_{i=1}^p [(\hat{w}_{i_{\zeta^*}}(\mathbf{x}) + \underline{\pi}_{i_{\zeta^*}}) \varpi_i(\mathbf{x}) + (\bar{\pi}_{i_{\zeta^*}} - \underline{\pi}_{i_{\zeta^*}}) Y_{2i}(\mathbf{x})], \quad (28)$$

$$\underline{M}_{\varpi}(\mathbf{x}) = \sum_{\zeta^*=1}^{\sigma^*} \varphi_{\zeta^*}(\mathbf{x}) \sum_{s=1}^p [(\hat{m}_{s_{\zeta^*}}(\mathbf{x}) + \bar{\phi}_{s_{\zeta^*}}) \varpi_s(\mathbf{x}) + (\underline{\phi}_{s_{\zeta^*}} - \bar{\phi}_{s_{\zeta^*}}) Y_{3s}(\mathbf{x})], \quad (29)$$

$$\overline{M}_{\varpi}(\mathbf{x}) = \sum_{\zeta^*=1}^{\sigma^*} \varphi_{\zeta^*}(\mathbf{x}) \sum_{s=1}^p [(\hat{m}_{s_{\zeta^*}}(\mathbf{x}) + \underline{\phi}_{s_{\zeta^*}}) \varpi_s(\mathbf{x}) + (\bar{\phi}_{s_{\zeta^*}} - \underline{\phi}_{s_{\zeta^*}}) Y_{4s}(\mathbf{x})]. \quad (30)$$

226 where  $Y_{1i}(\mathbf{x})$ ,  $Y_{2i}(\mathbf{x})$ ,  $Y_{3s}(\mathbf{x})$  and  $Y_{4s}(\mathbf{x})$  are positive decision variables which should satisfy  $Y_{1i}(\mathbf{x}) \geq \varpi_i(\mathbf{x})$ ,  $Y_{2i}(\mathbf{x}) \geq$   
 227  $\varpi_i(\mathbf{x})$ ,  $Y_{3s}(\mathbf{x}) \geq \varpi_s(\mathbf{x})$  and  $Y_{4s}(\mathbf{x}) \geq \varpi_s(\mathbf{x})$ .

228 Then the following inequation holds:

$$\frac{\underline{W}_{\varpi}(\mathbf{x})}{\underline{M}_{\varpi}(\mathbf{x})} \leq \frac{\sum_{i=1}^p w_i(\mathbf{x}) \lambda^T \mathbf{B}_i(\mathbf{x}) \mathbf{e}_m}{\sum_{s=1}^p m_s(\mathbf{x}) \lambda^T \mathbf{B}_s(\mathbf{x}) \mathbf{e}_m} \leq \frac{\overline{W}_{\varpi}(\mathbf{x})}{\overline{M}_{\varpi}(\mathbf{x})} \quad (31)$$

229 Thus, if  $f_{\min} \leq \frac{\underline{W}_{\varpi}(\mathbf{x})}{\underline{M}_{\varpi}(\mathbf{x})}$  and  $\frac{\overline{W}_{\varpi}(\mathbf{x})}{\overline{M}_{\varpi}(\mathbf{x})} \leq f_{\max}$  are satisfied, the condition (22) can be guaranteed. In addition, since  
 230 the membership-function-dependent terms  $\underline{W}_{\varpi}(\mathbf{x})$ ,  $\overline{M}_{\varpi}(\mathbf{x})$ ,  $\overline{W}_{\varpi}(\mathbf{x})$  and  $\underline{M}_{\varpi}(\mathbf{x})$  should **be** satisfied in every state  
 231 subspace instead of global state space, it is more relaxed to introduce the boundary information of the state subspace

232 into above inequation constraint conditions. So the constraint conditions  $f_{min} \leq \frac{W_{\varpi}(\mathbf{x})}{M_{\varpi}(\mathbf{x})}$  and  $\frac{\overline{W}_{\varpi}(\mathbf{x})}{\overline{M}_{\varpi}(\mathbf{x})} \leq f_{max}$  can be  
 233 relaxed as follows:

$$\underline{M}_{\varpi}(\mathbf{x}) - \sum_{\zeta^*=1}^{\sigma^*} \varphi_{\zeta^*}(\mathbf{x})\xi(\mathbf{x})R_{1\zeta^*} > 0 \quad (32)$$

$$\underline{W}_{\varpi}(\mathbf{x}) - f_{min}\overline{M}_{\varpi}(\mathbf{x}) - \sum_{\zeta^*=1}^{\sigma^*} \varphi_{\zeta^*}(\mathbf{x})\xi(\mathbf{x})R_{2\zeta^*} \geq 0, \quad (33)$$

$$f_{max}\underline{M}_{\varpi}(\mathbf{x}) - \overline{W}_{\varpi}(\mathbf{x}) - \sum_{\zeta^*=1}^{\sigma^*} \varphi_{\zeta^*}(\mathbf{x})\xi(\mathbf{x})R_{3\zeta^*} \geq 0, \quad (34)$$

234 where  $\xi(\mathbf{x}) = \sum_{o=1}^{\hat{n}} (x_{o\zeta^*} - x_{o\zeta^* \min})(x_{o\zeta^* \max} - x_{o\zeta^*})(\mathbf{x})$ ,  $x_{o\zeta^* \min}$  and  $x_{o\zeta^* \max}$  are the minimum and maximum values of  
 235 the system state variable  $x_o$  when it satisfies  $x_o \in \Psi_{\zeta^*}$ , so they carry boundary information of the state subspace;  $R_{1\zeta^*}$ ,  
 236  $R_{2\zeta^*}$  and  $R_{3\zeta^*}$  are the positive decision scalars which are used to assist in introducing boundary information of the state  
 237 subspace through the S-procedure. It should be noted that  $\overline{M}_{\varpi}(\mathbf{x}) > 0$  naturally holds due to  $\sum_{s=1}^p m_s(\mathbf{x})\varpi_s(\mathbf{x}) > 0$ ,  
 238 so only the constraint condition  $\underline{M}_{\varpi}(\mathbf{x}) > 0$  is set, but no constraint condition is set for  $\overline{M}_{\varpi}(\mathbf{x})$ .

239 Based on the definitions of  $\underline{W}_{\varpi}(\mathbf{x})$ ,  $\overline{W}_{\varpi}(\mathbf{x})$ ,  $\underline{M}_{\varpi}(\mathbf{x})$ , and  $\overline{M}_{\varpi}(\mathbf{x})$  in (27)-(30), the equivalent conditions of  
 240 inequalities (32)-(34) can be obtained:

$$\begin{aligned} & \Xi_{1\zeta^*}(\mathbf{x}) \\ &= \sum_{s=1}^p [(\hat{m}_{s\zeta^*}(\mathbf{x}) + \overline{\phi}_{s\zeta^*})\varpi_s(\mathbf{x}) + (\underline{\phi}_{s\zeta^*} - \overline{\phi}_{s\zeta^*})Y_{4s}(\mathbf{x})] - \sum_{o=1}^{\hat{n}} (x_{o\zeta^*} - x_{o\zeta^* \min})(x_{o\zeta^* \max} - x_{o\zeta^*})R_{1\zeta^*}(\mathbf{x}) > 0, \end{aligned} \quad (35)$$

$$\begin{aligned} & \Xi_{2\zeta^*}(\mathbf{x}) \\ &= \sum_{i=1}^p [(\hat{w}_{i\zeta^*}(\mathbf{x}) + \overline{\pi}_{i\zeta^*})\varpi_i(\mathbf{x}) + (\underline{\pi}_{i\zeta^*} - \overline{\pi}_{i\zeta^*})Y_{2i}(\mathbf{x})] - f_{min} \sum_{s=1}^p [(\hat{m}_{s\zeta^*}(\mathbf{x}) + \underline{\phi}_{s\zeta^*})\varpi_s(\mathbf{x}) + (\overline{\phi}_{s\zeta^*} - \underline{\phi}_{s\zeta^*})Y_{3s}(\mathbf{x})] \\ & \quad - \sum_{o=1}^{\hat{n}} (x_{o\zeta^*} - x_{o\zeta^* \min})(x_{o\zeta^* \max} - x_{o\zeta^*})R_{2\zeta^*}(\mathbf{x}) \geq 0, \end{aligned} \quad (36)$$

$$\begin{aligned} & \Xi_{3\zeta^*}(\mathbf{x}) \\ &= f_{max} \sum_{s=1}^p [(\hat{m}_{s\zeta^*}(\mathbf{x}) + \overline{\phi}_{s\zeta^*})\varpi_s(\mathbf{x}) + (\underline{\phi}_{s\zeta^*} - \overline{\phi}_{s\zeta^*})Y_{4s}(\mathbf{x})] - \sum_{i=1}^p [(\hat{w}_{i\zeta^*}(\mathbf{x}) + \underline{\pi}_{i\zeta^*})\varpi_i(\mathbf{x}) + (\overline{\pi}_{i\zeta^*} - \underline{\pi}_{i\zeta^*})Y_{2i}(\mathbf{x})] \\ & \quad - \sum_{o=1}^{\hat{n}} (x_{o\zeta^*} - x_{o\zeta^* \min})(x_{o\zeta^* \max} - x_{o\zeta^*})R_{3\zeta^*}(\mathbf{x}) \geq 0. \end{aligned} \quad (37)$$

241

## 242 **Part II: Positive Analysis**

243 Combined with the inequality form of input saturation (4) and the level set of linear copositive Lyapunov function  
 244 (8), the closed-loop system can be represented as follows:

$$\begin{aligned} \dot{\mathbf{x}} &= \sum_{i=1}^p w_i(\mathbf{x})(\mathbf{A}_i(\mathbf{x})\mathbf{x} + \mathbf{B}_i \text{sat}(\mathbf{u})) \\ &\geq \sum_{i=1}^p w_i(\mathbf{x})\mathbf{A}_i(\mathbf{x})\mathbf{x} + \sum_{i=1}^p w_i(\mathbf{x}) \sum_{k=1}^m \mathbf{B}_i^{(:,k)}(\mathbf{x}) \min\{u_{lim}, \sum_{j=1}^p m_j(\mathbf{x})\mathbf{G}_j^{(k,:)}(\mathbf{x})\mathbf{x}\} \end{aligned}$$

$$\begin{aligned}
 &= \sum_{i=1}^p w_i(\mathbf{x})\mathbf{A}_i(\mathbf{x})\mathbf{x} + \min_{1 \leq l \leq 2^m} \left\{ \sum_{i=1}^p \sum_{j=1}^p w_i(\mathbf{x})m_j(\mathbf{x})[u_{lim}\mathbf{B}_i(\mathbf{x})\mathbf{D}_l\mathbf{e}_m + \mathbf{B}_i(\mathbf{x})\mathbf{D}_l^-\mathbf{G}_j(\mathbf{x})\mathbf{x}] \right\} \\
 &\geq \min_{1 \leq l \leq 2^m} \left\{ \sum_{i=1}^p \sum_{j=1}^p w_i(\mathbf{x})m_j(\mathbf{x})[\mathbf{A}_i(\mathbf{x}) + u_{lim}\mathbf{B}_i(\mathbf{x})\mathbf{D}_l\mathbf{e}_m\lambda^T + \mathbf{B}_i(\mathbf{x})\mathbf{D}_l^-\mathbf{G}_j(\mathbf{x})\mathbf{x}] \right\} \quad (38)
 \end{aligned}$$

245 In order to ensure that the system states are always stay in the positive orthant, the derivative of the state reaching  
 246 the boundary needs to be non-negative, i.e.,  $\dot{x}_i \geq 0$  when  $x_i = 0$ . Thus, the positivity condition can be obtained as  
 247 follows:

$$\sum_{\beta: \beta \neq \alpha \in \underline{n}} [\mathbf{A}_i^{(\alpha, \beta)}(\mathbf{x}) + u_{lim}(\mathbf{B}_i(\mathbf{x})\mathbf{D}_l\mathbf{e}_m)^{(\alpha, \cdot)}(\lambda^T)^{(\cdot, \beta)} + (\mathbf{B}_i(\mathbf{x})\mathbf{D}_l^-)^{(\alpha, \cdot)}\mathbf{G}_j^{(\cdot, \beta)}(\mathbf{x})\mathbf{x}^{(\beta)}] \geq 0, \forall \alpha \in \underline{n}, l \in \underline{2^m}. \quad (39)$$

248 In order to unify the forms of the decision variables in the stability conditions and positivity conditions,  $\mathbf{G}_j(\mathbf{x})$   
 249 in the above conditions should be replaced with  $\frac{\mathbf{O}_j(\mathbf{x})}{\sum_{s=1}^p m_s(\mathbf{x})\lambda^T\mathbf{B}_s(\mathbf{x})\mathbf{e}_m}$ . Since  $\lambda > 0, \mathbf{B}_i(\mathbf{x}) > 0, \mathbf{e}_m > 0$ , we have  
 250  $\sum_{s=1}^p m_s(\mathbf{x})\lambda^T\mathbf{B}_s(\mathbf{x})\mathbf{e}_m > 0$ . Therefore, the positive condition for the polynomial fuzzy closed-loop system (2) is:

$$\begin{aligned}
 &\sum_{s=1}^p m_s(\mathbf{x}) \sum_{\beta: \beta \neq \alpha \in \underline{n}} [\lambda^T\mathbf{B}_s(\mathbf{x})\mathbf{e}_m\mathbf{A}_i^{(\alpha, \beta)}(\mathbf{x}) + \lambda^T\mathbf{B}_s(\mathbf{x})\mathbf{e}_mu_{lim}(\mathbf{B}_i(\mathbf{x})\mathbf{D}_l\mathbf{e}_m)^{(\alpha, \cdot)}(\lambda^T)^{(\cdot, \beta)} + (\mathbf{B}_i(\mathbf{x})\mathbf{D}_l^-)^{(\alpha, \cdot)}\mathbf{O}_j^{(\cdot, \beta)}(\mathbf{x})\mathbf{x}^{(\beta)}] \\
 &\quad \mathbf{x}^{(\beta)} \geq 0, \forall \alpha \in \underline{n} \quad (40)
 \end{aligned}$$

251 **Lemma 3.** There always exists a parameter  $\check{\lambda}$  such that the following inequations hold:

$$\lambda^T\mathbf{B}_s(\mathbf{x})\mathbf{e}_m \geq \check{\lambda}\mathbf{e}_n^T\mathbf{B}_s(\mathbf{x})\mathbf{e}_m, \quad (41)$$

$$\sum_{\beta: \beta \neq \alpha \in \underline{n}} (\mathbf{B}_i(\mathbf{x})\mathbf{D}_l\mathbf{e}_m)^{(\alpha, \cdot)}(\lambda^T)^{(\cdot, \beta)}\mathbf{x}^{(\beta)} \geq \sum_{\beta: \beta \neq \alpha \in \underline{n}} (\mathbf{B}_i(\mathbf{x})\mathbf{D}_l\mathbf{e}_m)^{(\alpha, \cdot)}\check{\lambda}\mathbf{x}^{(\beta)}, \quad (42)$$

252 where  $\check{\lambda}$  is undecided scalar.  $\mathbf{e}_m \in \mathfrak{R}^{m \times 1}$  is a column vector with all elements being 1, and  $\mathbf{e}_n \in \mathfrak{R}^{n \times 1}$  is similar to  $\mathbf{e}_m$ .

253 **Proof 3.** This proof is similar to the proof of the Lemma 2, so it is omitted.

254 Following the similar convexification line of the nonconvex term  $-u_{lim}\lambda^T\mathbf{B}_i(\mathbf{x})\mathbf{D}_l\mathbf{e}_m\lambda^T\mathbf{x}$  in stability conditions, the  
 255 nonconvex positivity condition (40) can be transformed as the following convex condition based on Lemmas 1 and 3:

$$\begin{aligned}
 &\sum_{s=1}^p m_s(\mathbf{x}) \sum_{\beta: \beta \neq \alpha \in \underline{n}} [\lambda^T\mathbf{B}_s(\mathbf{x})\mathbf{e}_m\mathbf{A}_i^{(\alpha, \beta)}(\mathbf{x}) + \mathbf{e}_n^T\mathbf{B}_s(\mathbf{x})\mathbf{e}_mu_{lim}(\mathbf{B}_i(\mathbf{x})\mathbf{D}_l\mathbf{e}_m)^{(\alpha, \cdot)}(\gamma_2^2 - 2\gamma_2\check{\lambda}) + \\
 &\quad (\mathbf{B}_i(\mathbf{x})\mathbf{D}_l^-)^{(\alpha, \cdot)}\mathbf{O}_j^{(\cdot, \beta)}(\mathbf{x})\mathbf{x}^{(\beta)}] \geq 0, \forall \alpha \in \underline{n} \quad (43)
 \end{aligned}$$

256 Since  $m_s(\mathbf{x}) \geq 0, \forall s \in \underline{p}$ , and  $\mathbf{x}^{(\beta)} \geq 0, \forall \beta \in \underline{n}$ , the above positivity condition can be satisfied if the following  
 257 positivity conditions hold:

$$\begin{aligned}
 &\Theta_{ijsl}^{(\alpha, \beta)}(\mathbf{x}) = \lambda^T\mathbf{B}_s(\mathbf{x})\mathbf{e}_m\mathbf{A}_i^{(\alpha, \beta)}(\mathbf{x}) + \mathbf{e}_n^T\mathbf{B}_s(\mathbf{x})\mathbf{e}_mu_{lim}(\mathbf{B}_i(\mathbf{x})\mathbf{D}_l\mathbf{e}_m)^{(\alpha, \cdot)}(\gamma_2^2 - 2\gamma_2\check{\lambda}) + (\mathbf{B}_i(\mathbf{x})\mathbf{D}_l^-)^{(\alpha, \cdot)}\mathbf{O}_j^{(\cdot, \beta)}(\mathbf{x}) \\
 &\quad \geq 0, \forall \alpha \neq \beta \in \underline{n} \quad (44)
 \end{aligned}$$

258 **Remark 4.** In this paper, the level set of the linear copositive Lyapunov function is incorporated into the stability  
 259 conditions and positivity conditions without introducing the decision variable, which may be more relaxed because  
 260 it **removes** the traditional constraint that the level set must be included in region  $\{\mathbf{x} : \|\mathbf{H}\mathbf{x}\|_\infty \leq 1\}$ , where  $\mathbf{H}$   
 261 is auxiliary controller gain when the saturation function is represented by the convex hull representation. Also, to  
 262 reduce the computational complexity of the iterative algorithm [7], the nonconvex stability conditions and positivity  
 263 conditions are effectively handled by the proposed convexification strategy which contains the proposed lemmas, sector  
 264 nonlinear method and advanced Chebyshev MFD method, so that the controller gains and other decision variables  
 265 can be obtained by one-step calculation. In conclusion, the analysis method and convexification strategy proposed in  
 266 this paper provide less conservative results and simpler calculation **programs**.

### Part III: Maximization of DOA

If the stability conditions  $\mathbf{Y}_{ijl1}(\mathbf{x}) < 0$ ,  $\mathbf{Y}_{ijl2}(\mathbf{x}) < 0$ , constraint conditions (32), (33), (34) and positivity conditions (44) all are satisfied, the level set of Lyapunov function  $\mathbf{P}(\lambda)$  can be regarded as the DOA of the systems, but the level set should be optimized by the following condition to find the largest one:

$$\ell \Omega_R \subset \mathbf{P}(\lambda) \quad (45)$$

where  $\ell$  is the optimize parameter, reference set  $\Omega_R$  is set as the polyhedron set:  $\Omega_R := \text{co}\{\mathbf{x}_0^1, \mathbf{x}_0^2, \dots, \mathbf{x}_0^l\}$ , then the above condition means that every vertex of  $\Omega_R$  is contained within the region  $\mathbf{P}(\lambda)$ , i.e., the following condition holds:

$$\lambda^T \ell \mathbf{x}_0^r \leq 1 \iff \hat{\ell} = \frac{1}{\ell} \quad \hat{\ell} - \lambda^T \mathbf{x}_0^r \geq 0; \forall \mathbf{r} \in \underline{l}. \quad (46)$$

With the smallest  $\hat{\ell}$  being obtained, the largest region  $\mathbf{P}(\lambda)$  can be obtained as the least conservative estimation of the DOA.

## 4. STABILITY ANALYSIS WITH CHEBYSGEV MFDS

In order to further reduce the conservatism of the results in Theorem 1 and expand the estimated DOA of the closed-loop system (2), the advanced piecewise Chebyshev MFD approach, as discussed in the stability analysis part of the previous section, is used to handle the stability conditions (20) and (21) in this section.

The membership functions defined in stability conditions (20) and (21) are  $h_{ij}(\mathbf{x}) = w_i(\mathbf{x})m_j(\mathbf{x})$ , and  $h_{ij}(\mathbf{x})$  are also nonlinear functions. Similar to the previous section,  $h_{ij}(\mathbf{x})$  are approximated by the following piecewise Chebyshev approximation membership functions:

$$\hat{h}_{ij}(\mathbf{x}) = \sum_{\zeta^*=1}^{\sigma^*} \varphi_{\zeta^*}(\mathbf{x}) \left( c_{0ij\zeta^*}^* + \sum_{q_h=1}^{\kappa_{h\zeta^*}^*} c_{q_hij\zeta^*}^* \tau_{q_h}(\mathbf{x}) \right), \quad (47)$$

where  $\kappa_{h\zeta^*}^*$  is the maximum approximate order of  $h_{ij}(\mathbf{x})$  in state subspace  $\Psi_{\zeta^*}$ .  $\tau_{q_h}(\mathbf{x})$  is polynomial of order  $q_h$ ,  $c_{0ij\zeta^*}^*, c_{1ij\zeta^*}^*, \dots, c_{\kappa_{h\zeta^*}^*ij\zeta^*}^*$  are the polynomials coefficients optimized by Remez algorithm.

Denote the approximated sub-membership functions in state subspace  $\Psi_{\zeta^*}$  as  $\hat{h}_{ij\zeta^*}(\mathbf{x}) := c_{0ij\zeta^*}^* + \sum_{q_h=1}^{\kappa_{h\zeta^*}^*} c_{q_hij\zeta^*}^* \tau_{q_h}(\mathbf{x})$ ,

the approximation errors of  $h_{ij\zeta^*}(\mathbf{x})$  are defined as  $\Delta h_{ij\zeta^*}(\mathbf{x}) = h_{ij\zeta^*}(\mathbf{x}) - \hat{h}_{ij\zeta^*}(\mathbf{x})$ . The upper boundary and lower boundary of  $\Delta h_{ij\zeta^*}(\mathbf{x})$  are  $\bar{\delta}_{ij\zeta^*}$  and  $\underline{\delta}_{ij\zeta^*}$ , respectively. If there exist a positive slack vectors  $\mathbf{R}_{4\zeta^*}$ ,  $\mathbf{R}_{5\zeta^*}$  and positive decision vectors  $\mathbf{N}_{ijl1}(\mathbf{x})$ ,  $\mathbf{N}_{ijl2}(\mathbf{x})$  such that  $\mathbf{N}_{ijl1}(\mathbf{x}) \geq \mathbf{Y}_{ijl1}(\mathbf{x})$ ,  $\mathbf{N}_{ijl2}(\mathbf{x}) \geq \mathbf{Y}_{ijl2}(\mathbf{x})$ ,  $\forall i, j \in \underline{p}, l \in \underline{2}^m$  is satisfied, the stability conditions (20) and (21) can be relaxed as the following MFD stability conditions:

$$\sum_{i=1}^p [(\hat{h}_{ij\zeta^*}(\mathbf{x}) + \underline{\delta}_{ij\zeta^*}) \mathbf{Y}_{ijl1}^{(\alpha)}(\mathbf{x}) + (\bar{\delta}_{ij\zeta^*} - \underline{\delta}_{ij\zeta^*}) \mathbf{N}_{ijl1}^{(\alpha)}(\mathbf{x})] - \sum_{o=1}^{\hat{n}} (x_{o\zeta^*} - x_{o\zeta^* \min})(x_{o\zeta^* \max} - x_{o\zeta^*}) \mathbf{R}_{4\zeta^*}^{(\alpha)}(\mathbf{x}) \\ \forall i, j \in \underline{p}, l \in \underline{2}^m, \zeta^* \in \underline{\sigma}^*, \alpha \in \underline{n} \quad (48)$$

$$\sum_{i=1}^p [(\hat{h}_{ij\zeta^*}(\mathbf{x}) + \underline{\delta}_{ij\zeta^*}) \mathbf{Y}_{ijl2}^{(\alpha)}(\mathbf{x}) + (\bar{\delta}_{ij\zeta^*} - \underline{\delta}_{ij\zeta^*}) \mathbf{N}_{ijl2}^{(\alpha)}(\mathbf{x})] - \sum_{o=1}^{\hat{n}} (x_{o\zeta^*} - x_{o\zeta^* \min})(x_{o\zeta^* \max} - x_{o\zeta^*}) \mathbf{R}_{5\zeta^*}^{(\alpha)}(\mathbf{x}) \\ \forall i, j \in \underline{p}, l \in \underline{2}^m, \zeta^* \in \underline{\sigma}^*, \alpha \in \underline{n} \quad (49)$$

By replacing the sub-conditions n) and o) in Theorem 1 with the aforementioned MFD stability conditions and the constraint conditions on  $\mathbf{N}_{ijl1}(\mathbf{x})$ ,  $\mathbf{N}_{ijl2}(\mathbf{x})$ , we obtain the following theorem:

**Theorem 2.** The saturated polynomial fuzzy system (2) is asymptotically stable and remains non-negative in a maximum DOA if there exist vectors  $\lambda \in \mathfrak{R}^n$ , scalars  $\tilde{\lambda}$  and  $\check{\lambda}$ , polynomial matrices  $\tilde{\mathbf{L}}_{ji}(\mathbf{x}) \in \mathfrak{R}^n$  and  $\mathbf{O}_j(\mathbf{x}) \in \mathfrak{R}^{m \times n}$ , and positive polynomial scalars  $Y_{q_1}(\mathbf{x})$ ,  $Y_{q_2}(\mathbf{x})$  and  $R_{\hat{q}_s}(\mathbf{x})$ ,  $\forall q_1 \in \{1, 2\}$ ,  $q_2 \in \{3, 4\}$ ,  $\hat{q} \in \{1, 2, 3\}$ ,  $i, s \in \underline{p}$ ,  $\zeta^* \in \underline{\sigma}^*$ ,

294 and positive polynomial vectors  $\mathbf{R}_{4\zeta^*}(\mathbf{x})$ ,  $\mathbf{R}_{5\zeta^*}(\mathbf{x})$ ,  $\mathbf{N}_{ijl1}(\mathbf{x})$ , and  $\mathbf{N}_{ijl2}(\mathbf{x})$ ,  $\forall i, j \in \underline{p}, l \in \underline{2^m}, \zeta^* \in \underline{\sigma^*}$ , such that the  
 295 following SOS-based conditions are satisfied:

min  $\hat{\ell}$

s.t.a) Subequations a) – m) of (5);

b)  $v^T(\mathbf{R}_{4\zeta^*}(\mathbf{x}) - \vartheta_8(\mathbf{x}))v$  is SOS;  $\forall \zeta^* \in \underline{\sigma^*}$

c)  $v^T(\mathbf{R}_{5\zeta^*}(\mathbf{x}) - \vartheta_9(\mathbf{x}))v$  is SOS;  $\forall \zeta^* \in \underline{\sigma^*}$

d)  $v^T(\mathbf{N}_{ijl1}^{(\alpha)}(\mathbf{x}) - \mathbf{Y}_{ijl1}^{(\alpha)}(\mathbf{x}) - \vartheta_{10}(\mathbf{x}))v$  is SOS;  $\forall i, j \in \underline{p}, l \in \underline{2^m}, \alpha \in \underline{n}$

e)  $v^T(\mathbf{N}_{ijl2}^{(\alpha)}(\mathbf{x}) - \mathbf{Y}_{ijl2}^{(\alpha)}(\mathbf{x}) - \vartheta_{11}(\mathbf{x}))v$  is SOS;  $\forall i, j \in \underline{p}, l \in \underline{2^m}, \alpha \in \underline{n}$

f)  $v^T(\mathbf{N}_{ijl1}^{(\alpha)}(\mathbf{x}) - \vartheta_{12}(\mathbf{x}))v$  is SOS;  $\forall i, j \in \underline{p}, l \in \underline{2^m}, \alpha \in \underline{n}$

g)  $v^T(\mathbf{N}_{ijl2}^{(\alpha)}(\mathbf{x}) - \vartheta_{13}(\mathbf{x}))v$  is SOS;  $\forall i, j \in \underline{p}, l \in \underline{2^m}, \alpha \in \underline{n}$

h)  $-v^T\left(\sum_{i=1}^p[(\hat{h}_{ij\zeta^*}(\mathbf{x}) + \underline{\delta}_{ij\zeta^*})\mathbf{Y}_{ijl1}^{(\alpha)}(\mathbf{x}) + (\bar{\delta}_{ij\zeta^*} - \underline{\delta}_{ij\zeta^*})\mathbf{N}_{ijl1}^{(\alpha)}(\mathbf{x})] - \sum_{o=1}^{\hat{n}}(x_{o\zeta^*} - x_{o\zeta^* \min})(x_{o\zeta^* \max} - x_{o\zeta^*})\right) \times$

$\mathbf{R}_{4\zeta^*}^{(\alpha)}(\mathbf{x}) - \vartheta_{14}(\mathbf{x}))v$  is SOS;  $\forall i, j \in \underline{p}, l \in \underline{2^m}, \alpha \in \underline{n}, \zeta^* \in \underline{\sigma^*}$

i)  $-v^T\left(\sum_{i=1}^p[(\hat{h}_{ij\zeta^*}(\mathbf{x}) + \underline{\delta}_{ij\zeta^*})\mathbf{Y}_{ijl2}^{(\alpha)}(\mathbf{x}) + (\bar{\delta}_{ij\zeta^*} - \underline{\delta}_{ij\zeta^*})\mathbf{N}_{ijl2}^{(\alpha)}(\mathbf{x})] - \sum_{o=1}^{\hat{n}}(x_{o\zeta^*} - x_{o\zeta^* \min})(x_{o\zeta^* \max} - x_{o\zeta^*})\right) \times$

$\mathbf{R}_{5\zeta^*}^{(\alpha)}(\mathbf{x}) - \vartheta_{15}(\mathbf{x}))v$  is SOS;  $\forall i, j \in \underline{p}, l \in \underline{2^m}, \alpha \in \underline{n}, \zeta^* \in \underline{\sigma^*}$

j)  $v^T(\lambda^T \mathbf{B}_s(\mathbf{x}) \mathbf{e}_m - \check{\lambda} \mathbf{e}_n^T \mathbf{B}_s(\mathbf{x}) \mathbf{e}_m)v$  is SOS;  $\forall s \in \underline{p}$

k)  $v^T\left[\sum_{\beta: \beta \neq \alpha \in \underline{n}} (\mathbf{B}_i(\mathbf{x}) \mathbf{D}_l \mathbf{e}_m)^{(\alpha, \cdot)} (\lambda^T)^{(\cdot, \beta)} \mathbf{x}^{(\beta)} - \sum_{\beta: \beta \neq \alpha \in \underline{n}} (\mathbf{B}_i(\mathbf{x}) \mathbf{D}_l \mathbf{e}_m)^{(\alpha, \cdot)} \check{\lambda} \mathbf{x}^{(\beta)}\right]v$  is SOS;  $\forall i \in \underline{p}, l \in \underline{2^m}, \alpha, \beta \in \underline{n}$

l)  $v^T(\Theta_{ijsl}^{(\alpha, \beta)}(\mathbf{x}) - \vartheta_{16}(\mathbf{x}))v$  is SOS;  $\forall i, j, s \in \underline{p}, l \in \underline{2^m}, \alpha \neq \beta$

(50)

296 where  $\vartheta_1 \sim \vartheta_{16}(\mathbf{x})$  also are predetermined positive scalar polynomials, and other variables all have been described  
 297 in Theorem 1.

## 298 5. SIMULATION EXAMPLES

299 In this section, a numerical example and the lipoprotein metabolism and potassium ion transfer model are employed  
 300 to validate the theoretical results of this paper.

301 **Example 1.** The nonlinear positive system is modeled using a polynomial fuzzy modeling approach, resulting in a  
 302 polynomial fuzzy positive system with three fuzzy rules. The polynomial system matrix and the polynomial input matrix  
 303 are given as follows:

$$\begin{aligned} \mathbf{A}_1(x_1) &= \begin{bmatrix} -0.039 & 28.82 \\ 1 & -2 - x_1^2 - x_1 \end{bmatrix}, \mathbf{A}_2(x_1) = \begin{bmatrix} -0.037 & 26.71 \\ 0.80 & -4 - 1.20x_1^2 \end{bmatrix}, \\ \mathbf{A}_3(x_1) &= \begin{bmatrix} -0.033 & 22.07 \\ 1 & -2.05 - x_1^2 - x_1 \end{bmatrix}, \\ \mathbf{B}_1(x_1) &= \begin{bmatrix} 3.27 + 0.05x_1^2 \\ 0.05 \end{bmatrix}, \mathbf{B}_2(x_1) = \begin{bmatrix} 2.90 + 0.02x_1^2 \\ 0.05 \end{bmatrix}, \mathbf{B}_3(x_1) = \begin{bmatrix} 2.09 + 0.10x_1^2 \\ 0.05 \end{bmatrix}. \end{aligned} \quad (51)$$

304 The system is subject to input saturation limit of  $u_{lim} = 10$ , and the membership functions for the system are shown  
 305 below:

$$w_1(x_1) = 1 - \frac{1}{1 + \exp[-5(x_1 - 2.375)]}, w_3(x_1) = 1 - \frac{1}{1 + \exp[-5(x_1 - 3.625)]},$$

**Table 1**

The rule for selecting the approximation order

$\kappa_{F_{\zeta}}^*$	[0, 0.1)	[0.1, 0.6)	[0.6, 1]
order	0	2	4

**Table 2**

The maximum absolute approximation error of the nonsmooth function in different intervals(Algorithm 1)

Subspaces	$m_1(x_1)$	order	$m_2(x_1)$	order	$m_3(x_1)$	order
[0, 2)	$3.3307 \times 10^{-16}$	0	0	0	0	0
[2, 2.75)	$1.2990 \times 10^{-14}$	2	$4.7740 \times 10^{-15}$	2	0	0
[2.75, 3.25)	0	0	$3.3307 \times 10^{-16}$	0	0	0
[3.25, 4)	0	0	$1.4766 \times 10^{-14}$	2	$9.2149 \times 10^{-15}$	2
[4, 6]	0	0	0	0	$3.3307 \times 10^{-16}$	0

**Table 3**

The maximum absolute approximation error of the nonsmooth function in different intervals(Equal partitioning)

Interval	$m_1(\mathbf{x})$	$m_2(\mathbf{x})$	$m_3(\mathbf{x})$
[0, 1.2)	$3.3307 \times 10^{-16}$	0	0
[1.2, 2.4)	0.2759	0.2759	0
[2.4, 3.6)	0.1625	0.1463	0.1582
[3.6, 4.8)	0	0.3017	0.3037
[4.8, 6]	0	0	$3.3307 \times 10^{-16}$

$$w_2(x_1) = 1 - w_1(x_1) - w_3(x_1). \quad (52)$$

306 The system membership functions above are complicated, to minimize the implementation cost of the controller,  
 307 the polynomial fuzzy controller is designed based on the IPM concept, the membership functions for the controller are  
 308 chosen to be the following simple functions:

$$m_1(x_1) = \begin{cases} 0 & \text{if } x_1 > 2.75 \\ -\frac{1}{0.75}x_1 + \frac{2.75}{0.75} & \text{if } 2 \leq x_1 \leq 2.75 \\ 1 & \text{if } x_1 < 2 \end{cases}, m_3(x_1) = \begin{cases} 1 & \text{if } x_1 > 4 \\ \frac{1}{0.75}x_1 - \frac{3.25}{0.75} & \text{if } 3.25 \leq x_1 \leq 4 \\ 0 & \text{if } x_1 < 3.25 \end{cases},$$

$$m_2(x_1) = 1 - m_1(x_1) - m_3(x_1). \quad (53)$$

309 To validate the effectiveness of the proposed Algorithm 1, the Chebyshev approximation of membership functions  
 310 is performed using both the algorithm proposed in this paper and the method in reference [36]. The entire operating  
 311 range is set as  $x_1 \in [0, 6]$ . When the Algorithm 1 is used to approximate the membership functions, the parameter  $\rho$   
 312 is set to 0.5 and the rule for selecting the approximation order is shown in Table 1. The partitioned state subspaces,  
 313 maximum absolute approximation errors of the Chebyshev approximation functions in each state subspace, and the  
 314 approximation orders are presented in Table 2.

315 When the Chebyshev membership functions approximation method in [36] is used, the state space is evenly divided  
 316 into 5 state subspaces, and the approximation order in each state subspace is set to 2. The partitioned state subspaces  
 317 and the maximum absolute approximation error of the Chebyshev approximation functions in each state subspace  
 318 are presented in Table 3.

319 From Tables 2 and 3, it can be observed that the maximum absolute approximation error obtained by the method  
 320 in reference [36] is larger than the maximum absolute approximation error obtained by Algorithm 1 in this paper. This  
 321 indicates that the algorithm proposed in this paper provides better approximation results for non-smooth membership  
 322 functions than the approximation method in [36].  
 323

**Table 4** $\lambda$ ,  $\hat{\ell}$ ,  $\mathbf{O}_j$  of Theorem 1 and Theorem 2

	$\lambda$	$\hat{\ell}$	$\mathbf{O}_j$
Theorem 1	$\begin{bmatrix} 0.23 \\ 1.14 \end{bmatrix}$	0.23	$\mathbf{O}_1(x_1) = [-2.0281 \times 10^{-6}x_1^2 - 5.7010 \times 10^{-2}x_1 - 2.7577, 0.6235x_1^2 + 0.1615x_1 - 4.7365]$ $\mathbf{O}_2(x_1) = [-2.0284 \times 10^{-6}x_1^2 - 5.7010 \times 10^{-2}x_1 - 2.7577, 0.6235x_1^2 + 0.1615x_1 - 4.7365]$ $\mathbf{O}_3(x_1) = [-2.0284 \times 10^{-6}x_1^2 - 5.7010 \times 10^{-2}x_1 - 2.7577, 0.6235x_1^2 + 0.1615x_1 - 4.7365]$
Theorem 2	$\begin{bmatrix} 0.20 \\ 1.00 \end{bmatrix}$	0.20	$\mathbf{O}_1(x_1) = [0.5170x_1^2 - 1.8951x_1 - 2.0655, 0.6143x_1^2 + 1.8645 \times 10^{-3}x_1 - 4.1251]$ $\mathbf{O}_2(x_1) = [0.3472x_1^2 - 2.1053x_1 - 1.7024, 0.5370x_1^2 + 1.0445 \times 10^{-1}x_1 - 4.0512]$ $\mathbf{O}_3(x_1) = [0.1954x_1^2 - 2.0709x_1 - 1.8682, 0.4843x_1^2 + 8.3471 \times 10^{-2}x_1 - 4.0517]$

### 5.1. Simulation Parameter Settings

When Theorem 1 is applied to system (51), The parameters  $\vartheta_1 - \vartheta_{10}(\mathbf{x})$  in Theorem 1 are set as  $1 \times 10^{-3}$ ,  $\gamma_1 = 0.23$ ,  $\gamma_2 = 1 \times 10^{-3}$ ,  $f_{\min} = 0.92$ ,  $f_{\max} = 1.1$ ,  $\rho = 0.5$ ; both the polynomial fuzzy controller gains  $\mathbf{O}_j(\mathbf{x})$  and the undetermined matrixes  $Y_{1i}(\mathbf{x})$ ,  $Y_{2i}(\mathbf{x})$ ,  $Y_{3s}(\mathbf{x})$ ,  $Y_{4s}(\mathbf{x})$ ,  $R_{1\zeta^*}(\mathbf{x})$ ,  $R_{2\zeta^*}(\mathbf{x})$ ,  $R_{3\zeta^*}(\mathbf{x})$  are set to second-order polynomials dependent on  $x_1$ . Following Algorithm 1, the entire operating domain is partitioned into  $[0, 2)$ ,  $[2, 2.75)$ ,  $[2.75, 3.25)$ ,  $[3.25, 4)$ , and  $[4, 6]$  based on the breakpoints of the first-order derivative of the membership functions. Furthermore, inspired by reference [33], the reference set for the DOA is selected as  $\chi_R := \text{co}\{(\sin(\theta), \cos(\theta))\}$ ,  $\theta \in [0, \frac{\pi}{2}]$ , with  $\theta$  ranging from  $[0, \frac{\pi}{2}]$ . When  $\theta = \frac{\pi}{2}$ ,  $\hat{\ell}$  takes the minimum value, enabling the system to achieve the maximum DOA. Finally, the obtained polynomial fuzzy controller gains  $\mathbf{O}_j(\mathbf{x})$ , Lyapunov function variables  $\lambda$ , and  $\hat{\ell}$  are presented in the Table 4.

When Theorem 2 is applied to system (51), The parameters  $\vartheta_1 \sim \vartheta_{16}(\mathbf{x})$  in Theorem 2 are set as  $1 \times 10^{-3}$  and  $\gamma_1 = 0.20$ , the undetermined matrixes  $\mathbf{R}_{4\zeta^*}(\mathbf{x})$ ,  $\mathbf{R}_{5\zeta^*}(\mathbf{x})$ ,  $\mathbf{N}_{ij11}(\mathbf{x})$  and  $\mathbf{N}_{ij12}(\mathbf{x})$  are set to second-order polynomials dependent on  $x_1$ . Other parameters are set the same as in the simulations of Theorem 1. The polynomial fuzzy controller gains  $\mathbf{O}_j(\mathbf{x})$ , Lyapunov function variables  $\lambda$ , and  $\hat{\ell}$  obtained from the simulations are presented in Table 4.

### 5.2. Discussion and Explanation

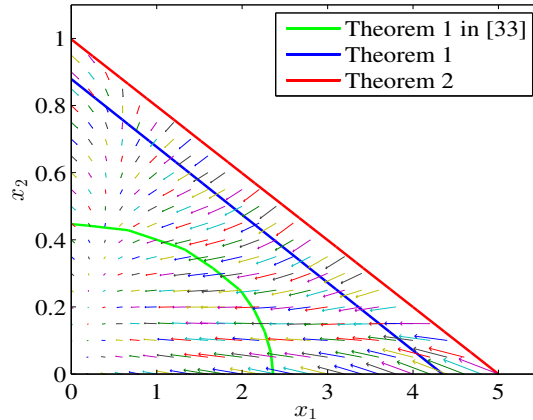


**Fig. 1:** Estimated DOAs for the polynomial fuzzy system are obtained using Theorems 1-2 in this paper and Theorem 1 in [33], along with a quiver plot.

The DOAs obtained by Theorems 1 and 2 in this paper, as well as the DOA obtained by Theorem 1 in reference [33], are drawn as red, blue, and green curves, respectively, in Fig. 1. When the approximation method in [36] is applied to perform MFD analysis for system (51), the approximate errors of the membership functions are so large that the analysis is too conservative, resulting in no feasible DOA being obtained. This indicates that Algorithm 1 proposed in this paper has stronger approximation ability than the approximation method in [36], and is more helpful to relax the conservatism of the results. The DOAs in Fig. 1 indicate that the novel analysis strategy and corresponding

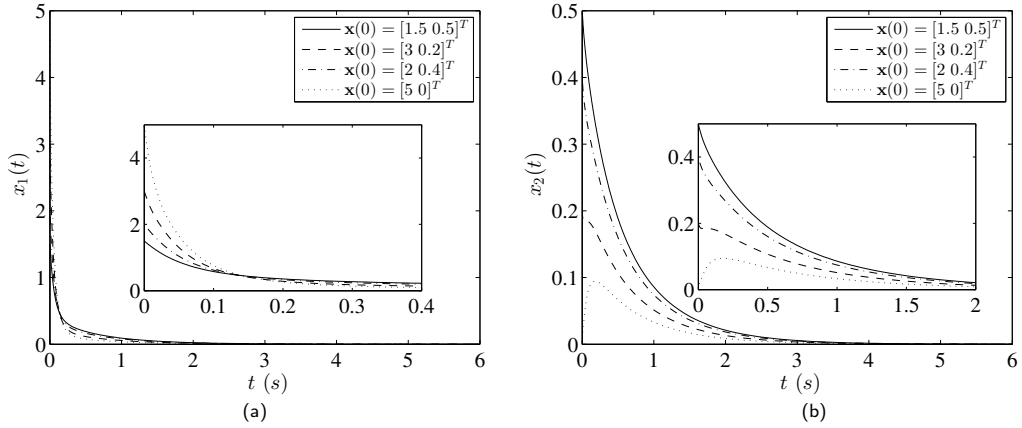


Fig. 2: The response curves of the system under different initial conditions

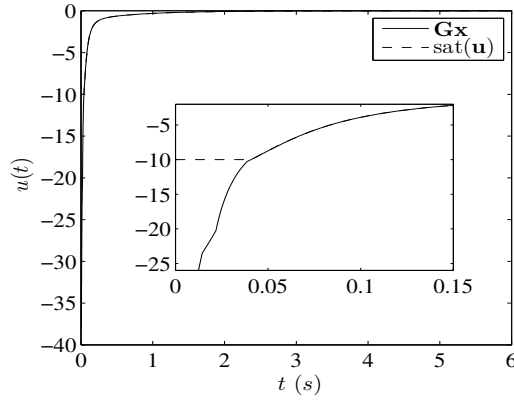


Fig. 3: The time response curve of the control input signal under the initial condition  $\mathbf{x}(0) = [5, 0]^T$ .

convexification strategy in this paper can expand the estimation of DOA more effectively than the analysis strategy based on the diagonal quadratic Lyapunov function and classical convex hull representation in [33]. Moreover, the application of the advanced Chebyshev MFD method to introduce membership functions information into stability conditions is helpful to further enlarge the estimation of DOA. Additionally, the quiver plots within the DOAs indicate that the initial states within all DOAs can be controlled to the origin by saturated control signals.

To provide a more intuitive display of the control performance of the polynomial fuzzy controller designed in this paper, the controller obtained by Theorem 2 is used to control the system (51). Four different initial conditions, denoted as  $\mathbf{x}(0) = [1.5, 0.5]^T$ ,  $\mathbf{x}(0) = [3, 0.2]^T$ ,  $\mathbf{x}(0) = [2, 0.4]^T$ , and  $\mathbf{x}(0) = [5, 0]^T$ , are selected, and the time responses of system states are shown in Fig. 2. When the initial condition is  $\mathbf{x}(0) = [5, 0]^T$ , the corresponding control inputs are shown in Fig. 3. In Fig. 3, the actual control input signal  $\mathbf{G}(\mathbf{x})\mathbf{x}$  and the saturated control input signal  $\text{sat}(\mathbf{u})$  are represented by solid and dashed lines, respectively. The control input signal  $\mathbf{G}(\mathbf{x})\mathbf{x}$  initially exceeds the saturation limit of 10 in Fig. 3, indicating that the system is subject to input saturation. The simulations above demonstrate that the polynomial fuzzy controller designed in this paper can drive the system states within the estimated DOA to the origin and keep them nonnegative.

**Example 2.** The lipoprotein metabolism and potassium ion transfer model can be represented by a general two-compartment model with arbitrary inputs (inflows) and outputs (excretions). This model can be described as the following nonlinear system:  $\dot{\mathbf{x}}(t) = \mathbf{A}(\mathbf{x}(t))\mathbf{x}(t) + \mathbf{B}(\mathbf{x}(t))\mathbf{u}(t)$ , where  $\mathbf{x}(t) = [x_1(t) \ x_2(t)]^T$  denote the material of corresponding compartment in mass units, respectively;  $\mathbf{u}(t) = [u_1(t) \ u_2(t)]^T$  denote the instantaneous rate of flow of material from outside the system (environment) into the corresponding compartment in units of mass/time. The system

363 matrix and input matrix are as follows:

$$\mathbf{A}(\mathbf{x}) = \begin{bmatrix} -0.2 - 0.07 \sin^2 x_1 & 0.83 \\ 1.65 & -0.2 \end{bmatrix}, \mathbf{B}(\mathbf{x}) = \begin{bmatrix} 0.6 + 0.07 \sin^2 x_1 & 0.1 \\ 0.5 & 0.1 \end{bmatrix}. \quad (54)$$

364 The lipoprotein metabolism and potassium ion transfer system (54) is open-loop unstable, meaning that the patient  
365 is unable to achieve normal autonomic metabolism due to functional failure. Next, a polynomial fuzzy controller is  
366 designed for the system (54) to treat the patient through the method proposed in this paper.

367 The nonlinear term  $0.07 \sin^2 x_1$  in system (54) can be expressed as  $0.07x_1 + 0.07(\sin^2 x_1 - x_1)$ . Define  $g(x_1) =$   
368  $0.07(\sin^2 x_1 - x_1)$ , employing sector nonlinear technique on  $g(x_1)$ , then it can be represented as follows:

$$g(x_1) = \tilde{w}_1(\mathbf{x})g_{\max} + \tilde{w}_2(\mathbf{x})g_{\min} \quad (55)$$

369 where  $\tilde{w}_1(\mathbf{x}) = \frac{g(x_1) - g_{\min}}{g_{\max} - g_{\min}}$  and  $\tilde{w}_2(\mathbf{x}) = 1 - \tilde{w}_1(\mathbf{x})$ ,  $g_{\max}$  and  $g_{\min}$  represent the maximum and minimum values of  $g(x_1)$   
370 over the operational domain, respectively.

371 The operational domain of the system state is set to  $x_1 \in [0, 6]$ , then  $g_{\min} = -0.4145$ ,  $g_{\max} = 0$ . Next, a polynomial  
372 fuzzy system with two rules can be used to describe the lipoprotein metabolism and potassium ion transfer system with  
373 input saturation limit 10, the system matrix and input matrix are as follows:

$$\mathbf{A}_1(\mathbf{x}) = \begin{bmatrix} -0.2 - 0.07x_1 & 0.83 \\ 1.65 & -0.2 \end{bmatrix}, \mathbf{A}_2(\mathbf{x}) = \begin{bmatrix} -0.2 - (0.07x_1 - 0.4145) & 0.83 \\ 1.65 & -0.2 \end{bmatrix},$$

$$\mathbf{B}_1(\mathbf{x}) = \begin{bmatrix} 0.6 + 0.07x_1 & 0.1 \\ 0.5 & 0.1 \end{bmatrix}, \mathbf{B}_2(\mathbf{x}) = \begin{bmatrix} 0.6 + 0.07x_1 - 0.4145 & 0.1 \\ 0.5 & 0.1 \end{bmatrix}. \quad (56)$$

374 The fuzzy controller of example 2 also is designed by IPM concept. The controller membership function  $m_1(\mathbf{x})$  is  
375 the same as (50), and  $m_2(\mathbf{x}) = 1 - m_1(\mathbf{x})$ .

### 376 5.1. Simulation Parameter Settings

377 When Theorem 1 is applied to system (56). The parameters  $\vartheta_1 - \vartheta_{10}(\mathbf{x})$  in Theorem 1 are set as  $1 \times 10^{-3}$ ,  $\gamma_1 =$   
378  $0.29$ ,  $\gamma_2 = 1 \times 10^{-3}$ ,  $f_{\min} = 0.92$ ,  $f_{\max} = 1.3$ ,  $\rho = 0.5$ ; both the polynomial fuzzy controller gains  $\mathbf{O}_j(\mathbf{x})$  and the undeter-  
379 mined matrixes  $\mathbf{Y}_{1i}(\mathbf{x})$ ,  $\mathbf{Y}_{2i}(\mathbf{x})$ ,  $\mathbf{Y}_{3s}(\mathbf{x})$ ,  $\mathbf{Y}_{4s}(\mathbf{x})$ ,  $\mathbf{R}_{1\zeta^*}(\mathbf{x})$ ,  $\mathbf{R}_{2\zeta^*}(\mathbf{x})$ ,  $\mathbf{R}_{3\zeta^*}(\mathbf{x})$  are set to second-order polynomials dependent  
380 on  $x_1$ . Following Algorithm 1, the entire operating domain is partitioned into  $[0, 2)$ ,  $[2, 2.75)$ ,  $[2.75, 3.25)$ ,  $[3.25, 4)$ ,  
381 and  $[4, 6]$  based on the breakpoints of the first-order derivative of the membership functions. Furthermore, inspired  
382 by reference [33], the reference set for the DOA is selected as  $\chi_R := \text{co}\{(\sin(\theta), \cos(\theta))\}$ ,  $\theta \in [0, \frac{\pi}{2}]$ , with  $\theta$  ranging  
383 from  $[0, \frac{\pi}{2}]$ . When  $\theta = \frac{\pi}{2}$ ,  $\hat{\ell}$  takes the minimum value, enabling the system to achieve the maximum DOA. Finally, the  
384 obtained polynomial fuzzy controller gains  $\mathbf{O}_j(\mathbf{x})$ , Lyapunov function variables  $\lambda$ , and  $\hat{\ell}$  are presented in the Table 5.

385 When Theorem 2 is applied to system (56). The parameters  $\vartheta_1 \sim \vartheta_{16}(\mathbf{x})$  in Theorem 2 are set as  $1 \times 10^{-3}$  and  
386  $\gamma_1 = 0.18$ , the undetermined matrixes  $\mathbf{R}_{4\zeta^*}(\mathbf{x})$ ,  $\mathbf{R}_{5\zeta^*}(\mathbf{x})$ ,  $\mathbf{N}_{ij11}(\mathbf{x})$  and  $\mathbf{N}_{ij12}(\mathbf{x})$  are set to second-order polynomials  
387 dependent on  $x_1$ . Other parameters are set the same as in the simulations of Theorem 1. The polynomial fuzzy controller  
388 gains  $\mathbf{O}_j(\mathbf{x})$ , Lyapunov function variables  $\lambda$ , and  $\hat{\ell}$  obtained from the simulations are presented in Table 5.

### 389 5.2. Discussion and Explanation

390 The DOAs obtained by Theorem 1 and Theorem 2 applied to the system (56) and the corresponding Quiver plot of  
391 states are shown in Fig. 4. From Fig. 4, it can be seen that the state points in the DOAs obtained by Theorem 1 and  
392 Theorem 2 can be controlled to the origin in a finite time and remain non-negative. In addition, the DOA obtained by  
393 Theorem 2 is larger than that obtained by Theorem 1, because the membership functions information is introduced  
394 into the stability conditions by the advanced Chebyshev MFD method in Theorem 2, which reduces the conservatism  
395 of the result.

396 To demonstrate the effectiveness of the proposed analysis strategies from another perspective, the polynomial  
397 fuzzy controller derived from Theorem 2 is used to control system (56). Four different initial conditions are selected:  
398  $\mathbf{x}(0) = [0, 3.9]^T$ ,  $\mathbf{x}(0) = [1, 2.5]^T$ ,  $\mathbf{x}(0) = [3, 1.5]^T$ , and  $\mathbf{x}(0) = [5.5, 0]^T$ . The time responses of system states are  
399 shown in Fig. 5. Fig. 6 illustrates the actual control input signal  $\mathbf{G}(\mathbf{x})\mathbf{x}$  and the saturated control input signal  $\text{sat}(\mathbf{u})$   
400 with solid and dashed lines, respectively. Both the actual control input signals  $\mathbf{G}(\mathbf{x})\mathbf{x}$  for  $u_1(t)$  and  $u_2(t)$  initially exceed

**Table 5**  
 $\lambda$ ,  $\hat{\ell}$ ,  $\mathbf{O}_j$  of Theorem 1 and Theorem 2

	$\lambda$	$\hat{\ell}$	$\mathbf{O}_j$
Theorem 1	$\begin{bmatrix} 0.29 \\ 0.41 \end{bmatrix}$	0.28	$\mathbf{O}_1(x_1) =$ $\begin{bmatrix} 1.6059 \times 10^{-7}x_1^2 - 1.1055 \times 10^{-2}x_1 - 0.8570, -8.4838 \times 10^{-7}x_1^2 - 5.6226 \times 10^{-5}x_1 - 0.2015 \\ -1.3453 \times 10^{-7}x_1^2 - 3.5821 \times 10^{-2}x_1 - 0.8810, -1.0491 \times 10^{-6}x_1^2 - 7.7454 \times 10^{-3}x_1 - 0.2883 \end{bmatrix}$ $\mathbf{O}_2(x_1) =$ $\begin{bmatrix} 1.6105 \times 10^{-7}x_1^2 - 1.1055 \times 10^{-2}x_1 - 0.8570, -8.4838 \times 10^{-7}x_1^2 - 5.6226 \times 10^{-2}x_1 - 0.2015 \\ -1.3377 \times 10^{-7}x_1^2 - 3.5821 \times 10^{-2}x_1 - 0.8810, -1.0491 \times 10^{-6}x_1^2 - 7.7454 \times 10^{-3}x_1 - 0.2883 \end{bmatrix}$
Theorem 2	$\begin{bmatrix} 0.18 \\ 0.26 \end{bmatrix}$	0.23	$\mathbf{O}_1(x_1) =$ $\begin{bmatrix} 3.4114 \times 10^{-2}x_1^2 - 9.0002 \times 10^{-2}x_1 - 0.4864, 4.1225 \times 10^{-2}x_1^2 - 1.0149 \times 10^{-1}x_1 - 0.1501 \\ 3.6644 \times 10^{-2}x_1^2 - 1.2945 \times 10^{-2}x_1 - 0.4732, 3.8971 \times 10^{-2}x_1^2 - 1.1503 \times 10^{-1}x_1 - 0.1649 \end{bmatrix}$ $\mathbf{O}_2(x_1) =$ $\begin{bmatrix} 8.0747 \times 10^{-3}x_1^2 - 8.7848 \times 10^{-2}x_1 - 0.4416, 5.9348 \times 10^{-3}x_1^2 - 5.1740 \times 10^{-2}x_1 - 0.0959 \\ 8.9110 \times 10^{-3}x_1^2 - 1.0878 \times 10^{-1}x_1 - 0.4117, 5.6635 \times 10^{-3}x_1^2 - 5.3008 \times 10^{-2}x_1 - 0.1049 \end{bmatrix}$

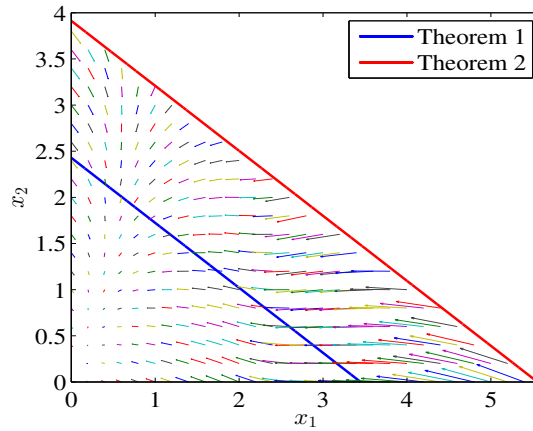


**Fig. 4:** Estimated DOAs for the polynomial fuzzy system are obtained using Theorems 1-2 in this paper , along with a quiver plot.

401 the saturated input limit of 10, indicating that the system is subject to input saturation constraints. The above simulation  
 402 results show that the polynomial fuzzy controller designed in this paper can effectively stabilize the system and keep  
 403 the system state non-negative, which means that the patient's metabolism can be restored to normal after treatment by  
 404 the polynomial fuzzy controller designed in this paper.

405

406 **Remark 5.** The algorithm proposed in this paper is a one-step calculation method, which has a lower computational  
 407 complexity compared to iterative calculation methods. When solving the conditions of Theorem 1 in a computer with  
 408 16G RAM and an i5-12400 CPU using MATLAB 2014a, Example 1 took 135 seconds and Example 2 took 97 seconds.  
 409 In contrast, the conditions of Theorem 2 took 1139 seconds for Example 1 and 931 seconds for Example 2. It is  
 410 evident that introducing membership function information increases computational complexity, but as shown in the  
 411 DOA comparison in Fig. 1 and 4, it effectively enlarges the DOA. Therefore, the algorithm in this paper is more suited  
 412 to customize mid-term or longer-term control strategies for systems.

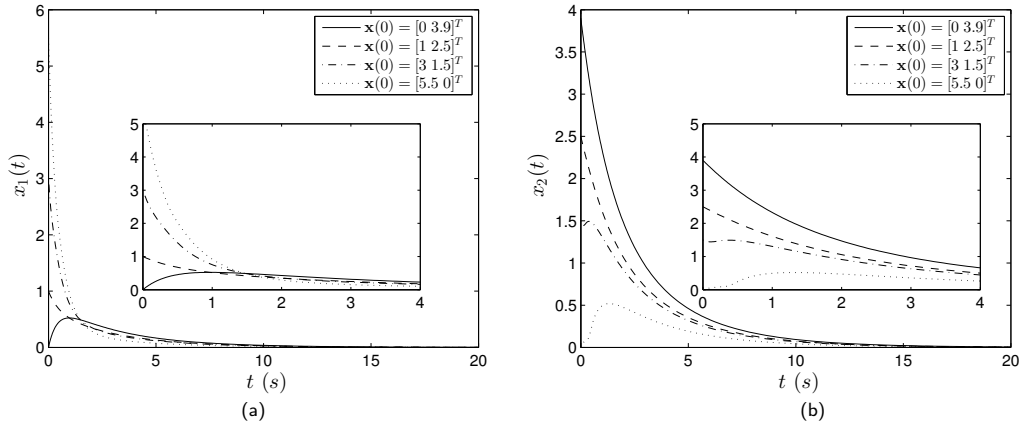


Fig. 5: The response curves of the system under different initial conditions

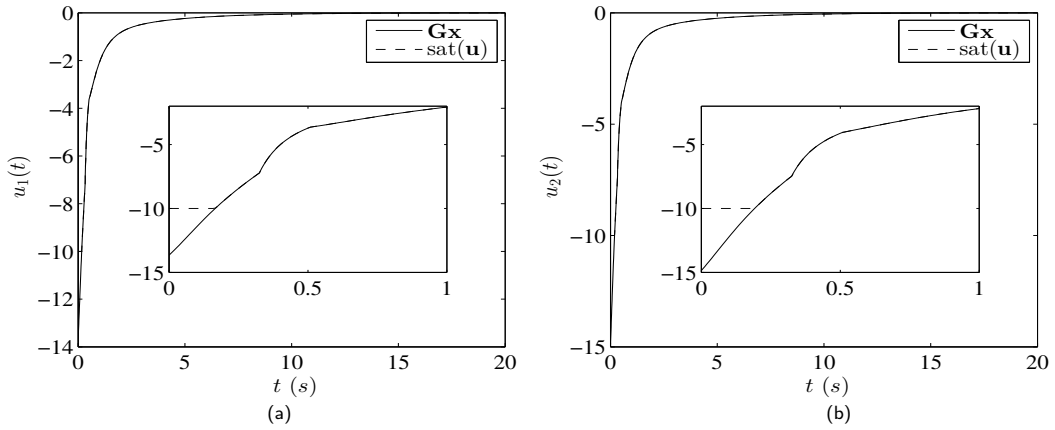


Fig. 6: The time response curve of the control input signal under the initial condition  $\mathbf{x}(0) = [5.5, 0]^T$ .

## 6. CONCLUSION

The DOA estimation has been investigated for the continuous-time positive polynomial fuzzy systems subject to input saturation in this paper. A novel analysis strategy based on inequality form of saturated function has been implemented to reduce the conservatism of the results. The non-convex problems encountered when the above analysis strategy are implemented on positive polynomial fuzzy systems have been solved by proposing some inequality lemmas and the advanced Chebyshev MFD method. Finally, the effectiveness and applicability of the novel analysis strategy and the convexification strategies in relaxing DOA estimation have been verified by a numerical example and the lipoprotein metabolism and potassium ion transfer system. In the future, we will investigate less conservative MFD methods and apply them to interval type-2 polynomial fuzzy models, thereby reducing control conservatism of nonlinear systems with uncertain parameters.

## Appendix A A novel Chebyshev Approximation Algorithm

**Algorithm 1** State space segmentation and approximation order selection algorithm.

**Step 1** Determine if all membership functions  $\mathbb{F}(\mathbf{x})$  are smooth functions. If they are, proceed to step 2; otherwise, go to step 3.

**Step 2** Divide the entire operating domain  $\Psi$  equally into " $\sigma^*$ " subdomains  $\Psi_{\sigma^*}$ . Proceed to Step 4.

**Step 3** Identify the breakpoints of the first-order derivative of all membership function  $\mathbb{F}(\mathbf{x})$  and divide the operating domain  $\Psi$  into " $\sigma^*$ " subdomains  $\Psi_{\zeta^*}$  based on these breakpoints.

**Step 4** Calculate the curvature of the membership function based on the following formula:

$$Curv_i = \max_{1 \leq r \leq n} \left\{ \frac{\left\| \frac{\partial^2 \mathbb{F}(\mathbf{x})}{\partial x_r^2} \right\|}{\left[ 1 + \left( \frac{\partial \mathbb{F}(\mathbf{x})}{\partial x_r} \right)^2 \right]^{3/2}}, \mathbb{F}(\mathbf{x}) \in \mathbb{F}(\mathbf{x}) \right\}$$

where  $\frac{\partial \mathbb{F}(\mathbf{x})}{\partial x_r}$  and  $\frac{\partial^2 \mathbb{F}(\mathbf{x})}{\partial x_r^2}$  are the first partial differential and second partial differential of the membership function  $\mathbb{F}(\mathbf{x})$  with respect to  $x_r$ , respectively.

**Step 5** Define the length of each subinterval as  $l_{\zeta^*}$ , and the maximum curvature in the subinterval  $\zeta^*$  is denoted as  $\max(Curv_i)_{\zeta^*}$  which means the maximum curvature for all the sample points. The approximation quality depends not only on the curvature of the function but also on the length of the approximation interval. Therefore, a convex combination of function curvature and interval length is used to determine the approximation order. Calculate the approximation order score  $\kappa_{\zeta}$  for each subinterval based on the following equation.

$$\kappa_{\mathbb{F}_{\zeta^*}}^* = \rho \frac{l_{\zeta^*}}{\sum_{\zeta^*=1}^{\sigma} l_{\zeta^*}} + (1 - \rho) \frac{\max(Curv_i)_{\zeta^*}}{\sum_{\zeta^*=1}^{\sigma} \max(Curv_i)_{\zeta^*}} \quad (\text{A-1})$$

where  $\rho$  ranges from 0 to 1, and a higher  $\rho$  value indicates that the interval length has a more significant impact on the approximation effect.

**Step 6** The approximate order in every subinterval is set according to the approximate order score  $\kappa_{\mathbb{F}_{\zeta^*}}^*$  obtained in Step 5. The order setting rule is that the larger the  $\kappa_{\mathbb{F}_{\zeta^*}}^*$ , the greater the order is set. The exact order setting depends on the calculation burden limits of the system.

## Appendix B Proof 2

**Proof 2.** The detailed presentations of  $\lambda^T \mathbf{x}$  and  $\mathbf{e}_n^T \mathbf{x}$  are  $[\lambda_1 \ \lambda_2 \ \dots \ \lambda_n] \times [x_1 \ x_2 \ \dots \ x_n]^T = \lambda_1 x_1 + \lambda_2 x_2 + \dots + \lambda_n x_n$  and  $\sum_{d=1}^n x_d$ , respectively. Then,  $\frac{\lambda^T \mathbf{x}}{\mathbf{e}_n^T \mathbf{x}} = \frac{x_1}{\sum_{d=1}^n x_d} \lambda_1 + \frac{x_2}{\sum_{d=1}^n x_d} \lambda_2 + \dots + \frac{x_n}{\sum_{d=1}^n x_d} \lambda_n$ . Due to  $\frac{x_1}{\sum_{d=1}^n x_d} + \frac{x_2}{\sum_{d=1}^n x_d} + \dots + \frac{x_n}{\sum_{d=1}^n x_d} = 1$ ,  $\frac{\lambda^T \mathbf{x}}{\mathbf{e}_n^T \mathbf{x}}$  is the convex combination of  $\lambda_1, \lambda_2, \dots, \lambda_n$ . So it can be concluded that there exists a parameter  $\tilde{\lambda}1$  with  $\lambda_{\min} \leq \tilde{\lambda}1 \leq \lambda_{\max}$  to make the inequation  $\frac{\lambda^T \mathbf{x}}{\mathbf{e}_n^T \mathbf{x}} \geq \tilde{\lambda}1$  holds, where  $\lambda_{\min}$  and  $\lambda_{\max}$  are the largest and smallest elements of vector  $\lambda$ . Moreover, the positive property of the positive system (2) implies that  $\mathbf{e}_n^T \mathbf{x} \geq 0$ , so the inequation (10) can be satisfied if  $\frac{\lambda^T \mathbf{x}}{\mathbf{e}_n^T \mathbf{x}} \geq \tilde{\lambda}1$  holds. Following the similar lines,  $\lambda^T \mathbf{B}_i(\mathbf{x}) \mathbf{D}_i \mathbf{e}_m \geq \tilde{\lambda}2 \mathbf{e}_n^T \mathbf{B}_i(\mathbf{x}) \mathbf{D}_i \mathbf{e}_m$  can be obtained, then there exists a parameter  $\tilde{\lambda} = \min\{\tilde{\lambda}1, \tilde{\lambda}2\}$  such that (10) and (11) hold.

## 7. ACKNOWLEDGEMENTS

The authors are grateful to the financial support of National Natural Science Foundation of China (62203094, 62203095, 62173079, U1808205), Natural Science Foundation of Hebei Province (F2023501021), Youth Foundation of Hebei Educational Committee (QN2023053), and Central University Basic Research Fund of China (N2223022, N2423027).

## References

- [1] X. Wang, Y. Tao, X. Song, Mathematical model for the control of a pest population with impulsive perturbations on diseased pest, Applied Mathematical Modelling 33 (7) (2009) 3099–3106.
- [2] S. Coogan, M. Arcak, A compartmental model for traffic networks and its dynamical behavior, IEEE Transactions on Automatic Control 60 (10) (2015) 2698–2703.
- [3] W. Haddad, V. Chellaboina, Q. Hui, Nonnegative and Compartmental Dynamical Systems, 2010.
- [4] L. Farina, S. Rinaldi, Positive linear systems: theory and applications, John Wiley & Sons, 2011.

- 464 [5] P. Wang, Y. Zhao,  $L_1$  reliable control for switched positive systems with actuator faults and state-dependent switchings, *Nonlinear Analysis: Hybrid Systems* 47 (2023) 101297.
- 465 [6] B. Zhu, J. Lam, M. Ogura, Log–log convexity of an optimal control problem for positive linear systems, *Automatica* 146 (2022) 110553.
- 466 [7] J. Shen, J. Lam, Analysis of positive systems with input saturation: Invariant hyperpyramids and hyperrectangles, *IEEE Transactions on Automatic Control* 67 (6) (2022) 3005–3012.
- 467 [8] D. E. Ghetmiri, A. A. Menezes, Control of positive systems with an unknown state-dependent power law input delay and input saturation, *Automatica* 151 (2023) 110853.
- 468 [9] J. Zhang, T. Raïssi, X. Deng, Indefinite krasovskii and razumikhin stability for nonlinear positive time-varying systems, *IEEE Transactions on Circuits and Systems II: Express Briefs* 69 (4) (2022) 2321–2325.
- 469 [10] X. Zhu, S. Liu, Y. Sun, Finite-time state bounding for homogeneous nonlinear positive systems with time-varying delay and bounded disturbance, *Journal of the Franklin Institute* 359 (6) (2022) 2681–2692.
- 470 [11] N. Zhang, Y. Kang, P. Yu, Stability analysis of discrete-time switched positive nonlinear systems with unstable subsystems under different switching strategies, *IEEE Transactions on Circuits and Systems II: Express Briefs* 68 (6) (2021) 1957–1961.
- 471 [12] S. Li, Z. Chen, Z. Xiang, Positivity and decentralized  $L_1$  control of nonlinear interconnected switched positive systems under MDDT constraint, *Nonlinear Analysis: Hybrid Systems* 50 (2023) 101410.
- 472 [13] T. Zhao, M. Huang, S. Dian, Robust stability and stabilization conditions for nonlinear networked control systems with network-induced delay via T-S fuzzy model, *IEEE Transactions on Fuzzy Systems* 29 (3) (2021) 486–499.
- 473 [14] K. Tanaka, H. Yoshida, H. Ohtake, H. O. Wang, A sum-of-squares approach to modeling and control of nonlinear dynamical systems with polynomial fuzzy systems, *IEEE Transactions on Fuzzy Systems* 17 (4) (2009) 911–922.
- 474 [15] E. Ahmadi, J. Zarei, R. Razavi-Far, Robust  $\ell_1$ -controller design for discrete-time positive T-S fuzzy systems using dual approach, *IEEE Transactions on Systems, Man, and Cybernetics: Systems* 52 (2) (2022) 706–715.
- 475 [16] L. Fu, H. K. Lam, F. Liu, H. Zhou, Z. Zhong, Robust tracking control of interval type-2 positive Takagi-Sugeno fuzzy systems with external disturbance, *IEEE Transactions on Fuzzy Systems* 30 (10) (2022) 4057–4068.
- 476 [17] J. Dong, Q. Hou, M. Ren, Control synthesis for discrete-time T-S fuzzy systems based on membership function-dependent  $H_\infty$  performance, *IEEE Transactions on Fuzzy Systems* 28 (12) (2020) 3360–3366.
- 477 [18] J. Ding, Y. Liu, J. Yu, X. Yang, Dissipativity-based integrated fault estimation and fault tolerant control for IT2 polynomial fuzzy systems with sensor and actuator faults, *IEEE Transactions on Fuzzy Systems* 31 (9) (2023) 2956–2965.
- 478 [19] X. Chen, L. Wang, M. Chen, J. Shen,  $\ell_\infty$ -induced output-feedback controller synthesis for positive nonlinear systems via T-S fuzzy model approach, *Fuzzy Sets and Systems* 385 (2020) 98–110.
- 479 [20] W. Qi, J. H. Park, J. Cheng, X. Chen, Stochastic stability and  $L_1$ -gain analysis for positive nonlinear semi-markov jump systems with time-varying delay via T-S fuzzy model approach, *Fuzzy Sets and Systems* 371 (2019) 110–122.
- 480 [21] P. Wang, D. Yang, Stability and  $L_1$ -gain analysis for switched positive fuzzy systems with time-delay: A state-dependent switching policy, *Fuzzy Sets and Systems* 464 (2023) 108440.
- 481 [22] J. Wang, J. Liang, A. M. Dobaie, Stability analysis and synthesis for switched Takagi-Sugeno fuzzy positive systems described by the roesser model, *Fuzzy Sets and Systems* 371 (2019) 25–39.
- 482 [23] H. K. Lam, A review on stability analysis of continuous-time fuzzy-model-based control systems: From membership-function-independent to membership-function-dependent analysis, *Engineering Applications of Artificial Intelligence* 67 (2018) 390–408.
- 483 [24] Y. Yu, H. K. Lam, K. Y. Chan, T-S fuzzy-model-based output feedback tracking control with control input saturation, *IEEE Transactions on Fuzzy Systems* 26 (6) (2018) 3514–3523.
- 484 [25] H. N. Nguyen, Further results on the control law via the convex hull of ellipsoids, *IEEE Transactions on Automatic Control* 69 (4) (2024) 2753–2760.
- 485 [26] J. Wang, J. Zhao, Stabilisation of switched positive systems with actuator saturation, *IET Control Theory & Applications* 10 (6) (2016) 717–723.
- 486 [27] Y. Li, Z. Lin, Improvements to the linear differential inclusion approach to stability analysis of linear systems with saturated linear feedback, *Automatica* 49 (3) (2013) 821–828.
- 487 [28] R. Ma, Q. Chen, S. Zhao, J. Fu, Dwell-time-based exponential stabilization of switched positive systems with actuator saturation, *IEEE Transactions on Systems, Man, and Cybernetics: Systems* 51 (12) (2021) 7685–7691.
- 488 [29] M. Han, H. K. Lam, F. Liu, Y. Tang, H. Zhou, Estimation of domain of attraction for discrete-time positive interval type-2 polynomial fuzzy systems with input saturation, *IEEE Transactions on Fuzzy Systems* 30 (2) (2022) 397–411.
- 489 [30] G. Yang, F. Hao, L. Zhang, B. Li, Actuator saturation control of continuous-time positive switched T-S fuzzy systems, *Journal of the Franklin Institute* 358 (17) (2021) 8862–8885.
- 490 [31] M. Han, H. K. Lam, F. Liu, Y. Tang, More relaxed stability analysis and positivity analysis for positive polynomial fuzzy systems via membership functions dependent method, *Fuzzy Sets and Systems* 432 (2022) 111–131.
- 491 [32] H. K. Lam, C. Liu, L. Wu, X. Zhao, Polynomial fuzzy-model-based control systems: Stability analysis via approximated membership functions considering sector nonlinearity of control input, *IEEE Transactions on Fuzzy Systems* 23 (6) (2015) 2202–2214.
- 492 [33] M. Han, H. K. Lam, F. Liu, L. Wang, Y. Tang, Stability analysis and estimation of domain of attraction for positive polynomial fuzzy systems with input saturation, *IEEE Transactions on Fuzzy Systems* 28 (8) (2020) 1723–1736.
- 493 [34] M. Narimani, H. K. Lam, SOS-based stability analysis of polynomial fuzzy-model-based control systems via polynomial membership functions, *IEEE Transactions on Fuzzy Systems* 18 (5) (2010) 862–871.
- 494 [35] A. Meng, H. K. Lam, Y. Yu, X. Li, F. Liu, Static output feedback stabilization of positive polynomial fuzzy systems, *IEEE Transactions on Fuzzy Systems* 26 (3) (2018) 1600–1612.
- 495 [36] Z. Bao, X. Li, H. K. Lam, Y. Peng, F. Liu, Membership-function-dependent stability analysis for polynomial-fuzzy-model-based control systems via Chebyshev membership functions, *IEEE Transactions on Fuzzy Systems* 29 (11) (2021) 3280–3292.

- 527 [37] L. Xie, C. E. De Souza, Robust  $H_\infty$  control for linear systems with norm-bounded time-varying uncertainty, IEEE Transactions on Automatic  
528 Control 37 (8) (1992) 1188–1191.